Research on fault-controlled hydrocarbon accumulation in rifted lacustrine basins based on structural geological modeling: a case study of the Banqiao area in Bohai Bay Basin, China

Yan Chen[1,2], Haitao Liu[2]*, Zhenglong Jiang[1], Jinghui Sun[3], Changyi Zhao[2], Wenya Jiang[4,5], Xiongying Dong[5] and Hongjun Li[2]

[1]School of Ocean Sciences, China University of Geosciences, Beijing, China, [2]Research Institute of Petroleum Exploration and Development, Beijing, China, [3]Beijing Institute of Geo-Environment Monitoring, Beijing, China, [4]College of Geosciences, China University of Petroleum, Beijing, China, [5]PetroChina Dagang Oilfield Company, Tianjin, China

The Banqiao area in the Bohai Bay Basin has experienced three stages of extensional deformation, leading to the formation of numerous fault-bound traps. Faults, acting as boundary conditions for these traps, play a crucial role in hydrocarbon accumulation. In this study, we conducted a 3D structural modeling of the area using high-resolution 3D seismic data and established a fault-reservoir database based on previous research. Our findings reveal four levels of faults in the Banqiao area: basin-controlling faults, boundary faults, derivative master faults, and secondary adjusting faults. The structural units can be categorized into subsag areas, slope areas, stress tran-sition zones, bifurcation and main incised fault zones, and southern block areas. The segmented growth of the main boundary faults controls the evolution of the subsags, with the subsidence center gradually shifting eastward from Rift Phase I to Rift Phase II, aligning with the distribution of source rocks. Fault-bound traps in the Banqiao area include single faults, intersecting faults, and side faults. Faults primarily act as barriers to lateral hydrocarbon migration during the process of hydrocarbon accumulation, while also providing pathways to a lesser extent. By integrating the fault-reservoir database with the fault system classification, we identified four types of fault-controlled hydro-carbon accumulation models: like-dipping fault barrier model, oppositely-dipping fault barrier model, intersecting fault barrier model, and reactivation-controlled secondary hydrocarbon ac-cumulation model. This structural geological model effectively demonstrates the spatial configura-tion of faults and their role in hydrocarbon accumulation in the Banqiao area. The fault control mechanisms presented in the model can also be applied to other blocks in the Bohai Bay Basin, laying a foundation for future petroleum exploration in continental rifted basins and facilitating the ap-plication of big data algorithms in various geoscientific research fields.

KEYWORDS

Banqiao area, structural geological modeling, database, fault-bound traps, fault-controlled hydrocarbon accumulation

1 Introduction

The formation and development of rifted lacustrine basins are controlled by the activity of the coeval major faults at the basin margins (Cukur et al., 2017; Deng et al., 2008; Wei et al., 2010; Zhao et al., 2015). During tectonic movements, when the applied tensile or compressive loads on crustal rock masses exceed their strength threshold, the rocks undergo brittle fracturing along fault planes, accompanied by significant displacements, leading to the formation of faults that maintain critical stress in the Earth's crust. The nonlinear accumulation of seismic activities results in complex structural characteristics of faulting with multidirectional superimposed deformations. This process generates numerous small fault clusters that adapt to the significant displacement variations around larger faults, forming a series of complex fault zones (John et al., 1991). These fault zones play a controlling role in the migration of underground fluids, including oil, gas, and water (Bense et al., 2013; Eichhubl et al., 2009; Etiope and Martinelli, 2002; Faulkner et al., 2010; Fu et al., 2013; Huang et al., 2016; Peng et al., 2018; Pfunt et al., 2016; Tang et al., 2009; Zelilidis et al., 2003).

Our understanding of faults has undergone a significant transformation throughout human history. Initially, faults were conceptualized as one-dimensional lines represented by two-dimensional Cartesian coordinates. Subsequently, this conception evolved into a three-dimensional fault plane devoid of thickness. However, recent developments have led to the recognition of faults as three-dimensional spatial structures with discernible thickness, known as deformation bands. Deformation bands are formed within highly porous rock formations and exhibit belt-like microstructures resulting from localized compaction, expansion, or shear-induced particle sliding, rotation, and fragmentation (Fossen, 2016; Schueller et al., 2013). These bands include various features, such as deformational breccia zones, deformation band shear zones (Davis, 1999), and small-scale faults (Fisher et al., 2003; Manzocchi et al., 1998). Advancements in GPS monitoring of active faults during the Neogene epoch have revealed the importance of considering small-scale temporal variations. As a consequence, the traditional perception of faults as "static" three-dimensional geometries has been replaced with a dynamic fault geometry that evolves over time (Clark Burchfiel et al., 2006; Dubbini et al., 2010). Exploiting the rapid progress in computer technology and mathematical modeling, researchers have integrated dynamic fault geometry with mechanical factors to enable fluid-solid coupling analysis. This integrated approach facilitates the evaluation of structural deformation within fault zones and its correlation with fluid migration (Schultz, 2019; Callahan et al., 2019; Fu et al., 2019; Hu et al., 2013). Complex fault systems exert significant control over fluid migration and fluid-solid coupling processes. This control arises from the presence of multiple orientations in regional faults. For instance, the main faults in the Qikou Depression of the Bohai Bay Basin exhibit two predominant orientations: NEE and nearly EW. These orientations give rise to structural transition zones, where the movement and interaction of fluids within the fault system have become a prominent research focus for experts and scholars globally (Fu et al., 2021; Liu, 2019; Liu, 2020). Liu et al. (2021) have conducted comprehensive studies using field surveys, remote sensing imagery, interpretation of exploration trenches, and relevant geophysical methods. Their research has yielded compelling

evidence of ancient seismic events and provided insights into their chronology. Additionally, they have introduced updated methodologies for exploring ancient seismic events, including the quantitative assessment of evidence grades and uncertainties. The findings of their study serve as fundamental data for elucidating the genesis of fault zones and estimating future earthquake probabilities. Importantly, their work has expanded the research scope and methodologies in this field, while contributing to the theoretical underpinnings of seismic reservoir formation (Luo and Huang, 2009; Yuan et al., 2013). Faulkner et al. (2010) conducted an analysis on brittle crust fault zones spanning approximately 10 years from 2000 to 2010. Using these fault zones as examples, they examined the structural characteristics of fault zones, the mechanical properties of fractures, the fluid mechanics within them, and their interrelationships. They proposed the viewpoint that tectonic and fluid-solid coupling are closely interconnected and should be evaluated together. In 2011, Faulkner et al. (2011) studied small-displacement fault zones and microfractured rock rupture areas in the Atacama region of northern Chile. They elucidated that the main manifestation of microfractured rupture zones is alteration halos surrounding the faults. Using the "a process zone" theory, they predicted that the width of fault damage zones increases with the length of the fault. This approach provides a better explanation for the extent of rupture areas around low-displacement faults. Yuan et al. (2020) introduced a mechanical method utilizing limit analysis to study the formation process of thrust faults in the upper crust during initial sliding. They found that, under appropriate overpressure conditions, the shape of the thrust fault is not significantly influenced by viscous or ductile deformation or regional stress rotation. Increasing the fluid viscosity coefficient and internal cohesion can significantly reduce the curvature and length of the thrust fault. This method was applied to the offshore areas of the Niger Delta and the northwestern Gulf of Mexico to validate the control of fluid pressure on thrust fault formation.

According to reports from major oil fields and previous research papers, it is evident that fault-related oil and gas reservoirs continue to play a significant role in the rift basins of eastern China (Fu et al., 2021; Gong et al., 2019; Chu et al., 2019; Zhao et al., 2016a). The structural analysis of fault systems in the oil-bearing areas of the Bohai Bay Basin has received considerable attention. The enhancement of research methods and technological means has further elevated the research level in this field. As a result, numerous innovative achievements have been made in studying the deformation characteristics of fault zones, fault sealing properties, and their relationship with fluid migration (Fu et al., 2021; Fu et al., 2015; Liu, 2019; Liu, 2020; Chu et al., 2019; Zhao et al., 2016a). During the process of fracture deformation, fault traps are formed in the hanging wall and footwall of rock formations in the oil-bearing areas. Among various trap types, fault traps are the most widespread in the Qikou Depression of the Bohai Bay Basin (Chu, 2019; Fu et al., 2021; Chu et al., 2019).

The Banqiao area is a secondary tectonic unit in the Neogene Qikou Depression of the Bohai Bay Basin, representing a typical faulted and subsided basin—a lake basin formed by crustal faulting and subsidence in geological history. Song et al. conducted detailed studies on the structural system, sediment sources, hydrodynamic environment, and contemporaneous fault activity in the Banqiao Depression, using core descriptions and well-seismic integration.

They proposed a sedimentary model applicable to the Banqiao area Song et al., (2016); Song et al., (2018). Liu et al. (2017) performed thermal decomposition experiments, stable carbon isotope analysis, and biomarker analysis on rock samples from the Banqiao area. They compared the experimental results with crude oil samples and classified the hydrocarbon source rocks of the Shahejie Formation, identifying Es1x and Es3 as two effective hydrocarbon source rocks. Wang and Yin, and others established fluid property discrimination charts using various methods such as resistivity imaging, pore structure analysis, and clay content correction, based on the analysis of well logging curves in the Banqiao area. They qualitatively determined the lower limit of effective reservoirs in the Banqiao area and reevaluated old wells. The results were verified with production data from appraisal wells in the slope area (Wang et al., 2018; Yin et al., 2019). Chen, Wang, and others analyzed the Es3 source rocks and reservoir properties and found that the Banqiao area has a developed low-slope sand body, with a combination of faults forming a unified drainage system. This led to the conclusion that the area has the potential to form deep, large-scale natural gas reservoirs. They identified the downdip slope area of the Dazhangtuo Fault as a favorable zone (Chen et al., 2013; Li, 2016). Zhou et al. used well-seismic integration and analysis of laboratory data to identify the distribution system of interbedded gray-black mudstones and sandstones in the Es1x subinterval in the Banqiao area. Targeted exploration deployment based on this research achieved good exploration results (Zhou et al., 2018). Wang, Chen, and others analyzed the tectonic-sedimentary evolution characteristics and favorable reservoir facies belts in the Banqiao area using seismic data, well logging, thin section identification, and oil-source correlation. They found that the Banqiao area experienced two stages of overall subsidence and rotation and identified the gentle slope as the structural background for lithological traps. The early gentle paleotopography favored the superposition and continuity of high-quality sand bodies in the gentle slope area, while the late rotation and uplift promoted the formation of steep-dip lithological traps (Chen et al., 2017; Wang et al., 2017).
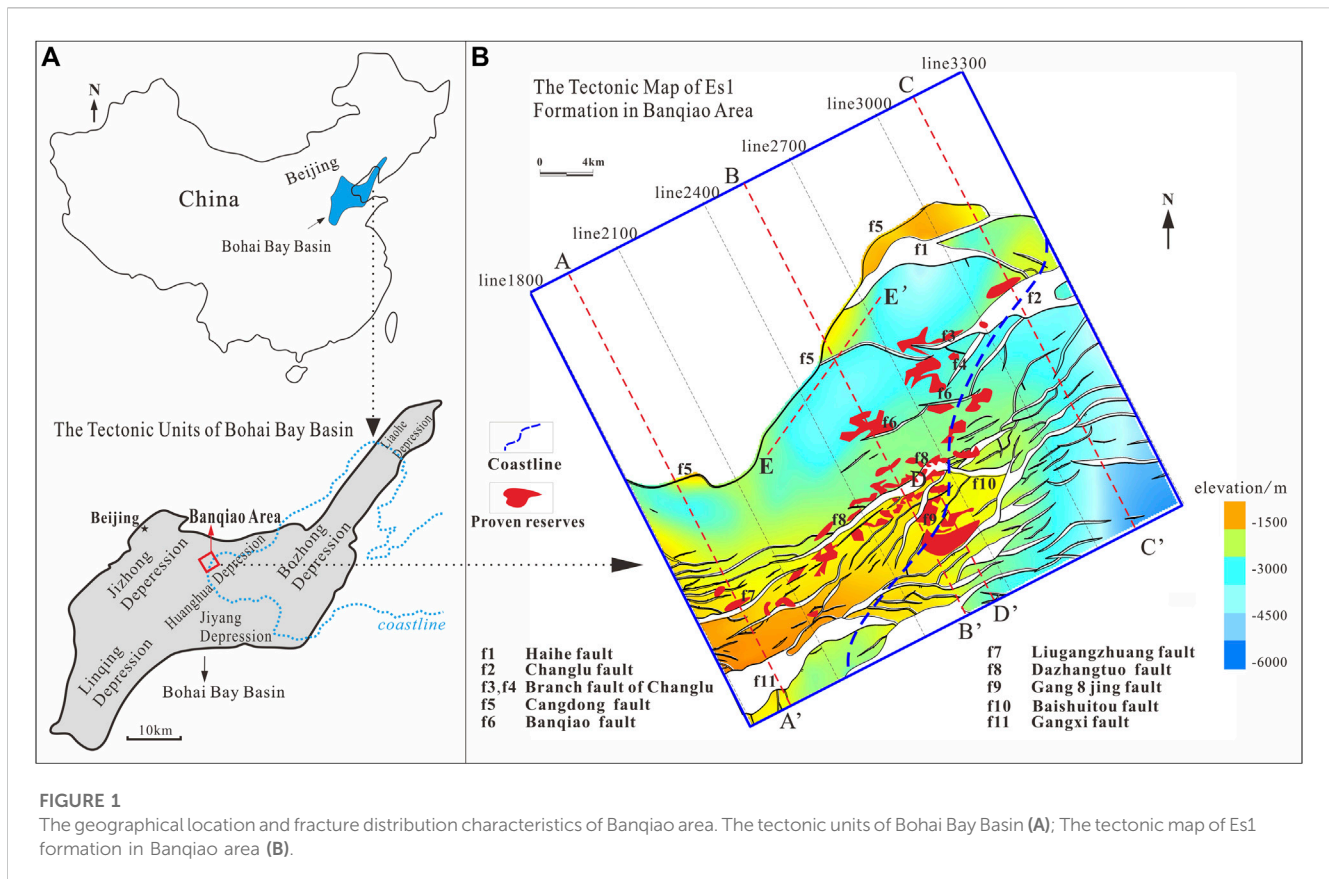
Chinese experts and scholars have conducted extensive research on the structures, sedimentation, and reservoirs in the Banqiao area. However, there is still a lack of detailed characterization of the impact of fault zones on hydrocarbon accumulation. In light of this, this study relies on abundant regional geological and three-dimensional seismic data to establish a three-dimensional model and geological database of the Banqiao area. It finely delineates structural units and explores the controlling role of faults on hydrocarbon accumulation in the faulted basin. The research findings will contribute to the theoretical understanding of fault-controlled hydrocarbon accumulation in continental basins, lay the foundation for data analysis and the transition to the era of big data in three-dimensional modeling of heterogeneous sources, and provide a basis for future hydrocarbon evaluation, exploration, and development in the region.

2 Geological setting

The Bohai Bay Basin is one of the largest onshore basins in northern China. Located in the seismically active zone of North China, the basin experiences frequent seismic activity. Throughout history, the basin has been subjected to significant earthquakes that have had a profound impact on its geological structure and the formation of its oil and gas resources (Xie, 2020). The Banqiao area, situated in the central part of the Bohai Bay Basin, is a secondary tectonic unit of the Cenozoic era. The area's complex fault system is the result of multiple phases of tectonic movement, controlled by various faults such as the Cangdong Fault in the west, the Haihe Fault in the north, the Dazhangtuo Fault in the central region, and the Gangxi Fault in the south (Figure 1). Currently, approximately one-third of the area is covered by the Bohai Sea, with water depths ranging from 0 to 5 m. The main feature of the Banqiao area is a large-scale, oil and gas rich rotation and tilting slope zone, which not only provides favorable conditions for the formation of structural oil and gas reservoirs but also facilitates the development of stratigraphic, lithological, and structural-lithological oil and gas traps (Zhao et al., 2016b). Since the industrial oil and gas flow was first achieved in the lower Es1 interval of Well B3 in 1973, continuous discoveries have been made. By 2017, three oil and gas fields, namely Dazhangtuo, Banqiao, and Baishuitou, have been discovered in the area. Studies have shown that the sandstone strata in the slope area of the Es3 interval have undergone high thermal evolution and have a strong gas generation capacity. They possess favorable conditions for the large-scale accumulation of continuous oil and gas resources. The low slope zone of Banqiao is a high-value area with a strong gas generation capacity, providing the resource foundation for the formation of large and medium-sized natural gas fields (Jia et al., 2021; Song et al., 2018). Significantly, major achievements have been made in the exploration of lithological oil and gas reservoirs in the slope area, with the discovery of four billion-ton scale reservoir zones. Explorations in the Paleozoic era have achieved important breakthroughs, opening up new prospects for hidden mountain exploration. Deep-seated natural gas exploration has also made significant progress, demonstrating promising exploration prospects (He et al., 2021; Liu, 2019).

The sedimentary formations in the Banqiao area are developed from bottom to top and include the Paleogene Shahejie Formation (Es3, Es2, Es1), Dongying Formation (Ed), Neogene Guantao Formation (Ng), and Minghuazhen Formation (Nm). This area is a key focus for exploration and development in the Dagang Oilfield (Figure 2). There are two sets of hydrocarbon source rocks in the Cenozoic, namely, the upper submember of the third member of the Shahejie Formation (Es3) and the lower submember of the first member of the Shahejie Formation (Es1). The Shahejie Formation Es3 interval is the first and most important source rock system within the basin, with a thickness of 400–1,400 m. It is a predominantly humic type organic-rich source rock with a high organic matter content of 0.6%–1.25% and high thermal maturity, typically with a Ro less than 1.2%. The Es1 interval of the Shahejie Formation is also a humic type source rock with a relatively high organic matter content and moderate thermal maturity, generally with a Ro below 0.7%. The reservoirs in the Banqiao area are mainly distributed within the Shahejie Formation, Dongying Formation, Guantao Formation, and Minghuazhen Formation. The extensive lateral distribution of sedimentary systems in the Banqiao area, resulting from multiple tectonic movements during the Cenozoic era, has facilitated the formation of intersecting and overlapping sand bodies that create high-porosity channels for hydrocarbon accumulation, providing effective storage space for oil and gas and

FIGURE 1
The geographical location and fracture distribution characteristics of Banqiao area. The tectonic units of Bohai Bay Basin **(A)**; The tectonic map of Es1 formation in Banqiao area **(B)**.

facilitating the formation of good reservoirs. The Banqiao area is characterized by the development of several regional sealing layers from bottom to top, including the middle part of the Es1, Ed2, and the middle part of the Nm formations, which predominantly consist of mudstone with strong sealing properties. The Shahejie Formation is characterized by the development of interbedded sand and mud layers. Taking the top of the Sha 3 Member as an example, even the thicker mudstone layers can serve as regional sealing layers (Wang, 2008). Different types of oil and gas accumulations are formed in the area due to differences in reservoir-seal combinations, hydrocarbon migration conditions, and other factors. These include self-generated and self-trapped accumulations in the Es3 member, self-generated and self-trapped as well as downward-migrated and upward-trapped accumulations in the Es2 member and lower Es1 member, self-generated and self-trapped as well as downward-migrated and upward-trapped accumulations in the middle Es1 member, upper Es1 member, and Ed formation, and downward-migrated and upward-trapped accumulations in the Neogene Ng formation and Nm formation (Wang et al., 2020).

3 Data and methodology

Geological simulation can be divided into two main categories: numerical simulation and physical simulation experiments. Physical simulation involves the use of materials such as quartz sand, clay, silt, silicone gel, and gelatin to analyze structural behavior through methods like stretching and compression. In particular,

photoelasticity materials, including transparent amorphous substances like gelatin and glass, are utilized for optical elasticity simulation. When subjected to loads and strain, these materials undergo a transition from isotropy to anisotropy in their spatial state. By observing the phenomenon of double refraction of light in these materials, interference images can be obtained to reflect the characteristics of stress distribution (Reber et al., 2020). In recent decades, the rapid development of mathematics and computers has facilitated the widespread application of numerical simulation in the field of geology. By setting parameters and adjusting computational results, numerical simulation enables the generation of stress contour maps for geological formations within idealized models. Due to its convenient computational process, high-quality results, and visually appealing visualization, numerical simulation has now largely replaced optical elasticity simulation experiments as the mainstream approach for stress field analysis. The commonly employed computational methods include finite element method, finite difference method, discrete element method, and others.

Basin modeling is an important tool in basin analysis and serves as a fundamental approach to systematically investigate the processes and mechanisms of basin formation (Bergen et al., 2019; Gurnis et al., 2018; Zhu, 2020; Zhu et al., 2021). Various methods are employed for basin reconstruction, including sediment provenance analysis, basin deformation reconstruction, sedimentary facies analysis, paleogeographic restoration, etc. (Zhu, 2020; Zhu et al., 2021). Basin analysis is gradually shifting from qualitative to quantitative approaches (Bergen et al., 2019; Gurnis et al., 2018). Quantitative determination of basin deformation can accurately
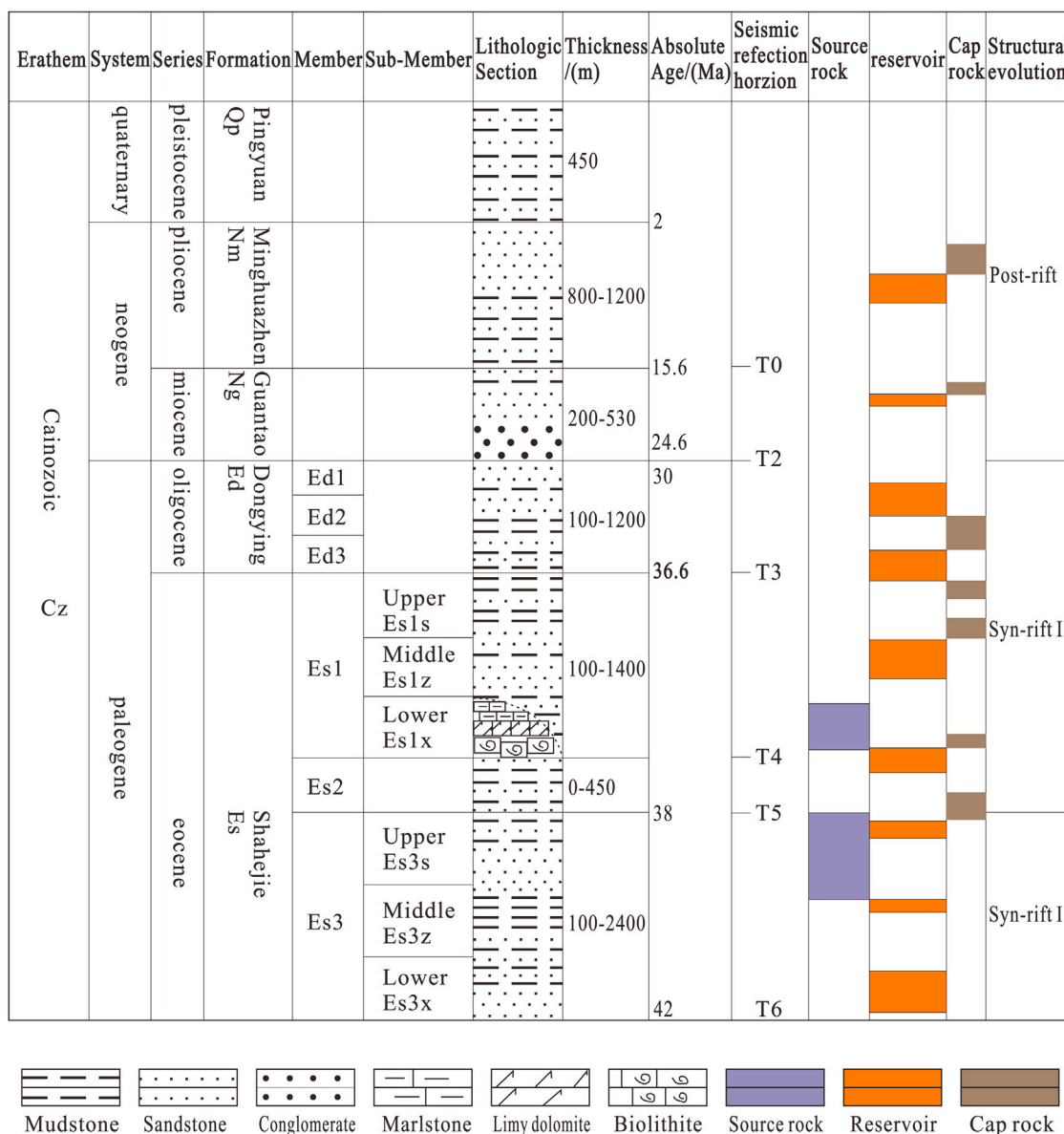
FIGURE 2
Schematic stratigraphic column for the Banqiao area, Bohai Bay Basin. Ed1, first member of the Dongying Formation; Ed2, second member of the Dongying Formation; Ed3, third member of the Dongying Formation; Es1, first member of the Shahejie Formation; Es2, second member of the Shahejie Formation; Es3, third member of the Shahejie Formation.

reflect the evolutionary history of the basin, providing significant insights into the study of basin formation and regional tectonic history. Moreover, it has practical applications in analyzing preferential pathways for hydrocarbon migration within fault zones and assessing fault seal capacity in actual production projects (Liu, 2019; Wang et al., 2020). Simultaneously, the establishment of an information database during modeling has been widely applied in various geological fields such as hydrocarbon-bearing basins, fault-controlled reservoirs, geological mapping for engineering purposes, and geological hazard prediction (Chen and Zhang, 2018; Wang et al., 2020; Wu et al., 2019; Zhou et al., 2007). Furthermore, it can serve as a valuable reference for future geological investigations, petroleum exploration, and other geoscientific research fields as they rapidly advance into the era of big data (Liu, 2022).

3.1 Data

The 3D seismic data set utilized in this study features a line spacing of 25 m (82 ft) in the southeast–northwest direction and is oriented southwest to northeast. For the Banqiao area, the Es3, Es2, Es1, Ed, Ng, and Nm members exhibits timemigrated volume frequencies ranging from 25 Hz to 30 Hz, providing a seismic resolution of approximately 10–15 m (32–49 ft). The estimation of throw values involves measuring the vertical components of
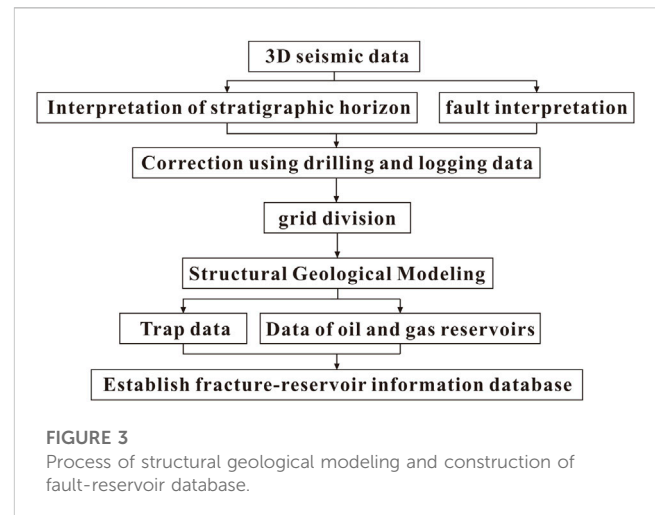
the total strata displacement vectors in milliseconds (i.e., the two-way travel time).

3.2 Hypothesis

Prior to modeling, the following assumptions are made regarding the idealized stratigraphy and faults: Each stratigraphic unit is treated as a homogeneous and continuous material, where the properties of a small rock sample are identical to any other small sample. Except at the fault-stratigraphy interface, the physical parameters such as density and Poisson's ratio are assumed to be uniform throughout the model. Transitions between interconnected stratigraphic units are smoothly continuous from uplift to subsidence. Recognizing that actual materials are never perfectly homogeneous, even the most homogeneous and seemingly tightly compacted quartzite cubes contain small fractures along grain boundaries. The entire stratigraphic sequence is assumed to comply with commonly used mechanical formulas such as Griffith's criterion for fracture and the Rankine failure criterion. The stratigraphic layers undergo sliding along the fault plane without causing any morphological or mechanical changes to the fault. The fault is idealized as a homogeneous fault plane without any thickness, tightly connected to the stratigraphy. Only the self-gravity of the stratigraphy and the internal tectonic stresses within the rock system are considered, while other external geological processes such as metamorphism, erosion, and transport during diagenesis are neglected. The influence of compaction during the sedimentation process on the mechanical properties of the stratigraphy is disregarded, and newly deposited layers are assumed to be nearly horizontal. Since no significant erosion events have occurred in the study area since the deposition of the Neogene sandstone interval (Liu, 2019), the erosional effects in the study area are ignored.

3.3 Methodology of Structural Geological modeling

The workflow for constructing a structural geological model is as follows (Figure 3): Firstly, the three-dimensional seismic data points and the interpreted data from contiguous processing are imported into the model. The data is organized, interpreted, and divided into different stratigraphic units, including the Shahejie Formation (Es3, Es2, Es1), Dongying Formation (Ed), Guantao Formation (Ng), and Minghuazhen Formation (Nm). Due to limitations in seismic resolution, the modeling focuses only on the identified major faults, while smaller and less recognizable faults are not delineated. Additionally, the assumed fault is idealized as a homogeneous fault plane without any thickness. Under the assumption that small-scale faults do not develop and the stratigraphy is treated as a continuous medium, the main faults are named and a simplified model is created. Next, the gaps in the stratigraphy and faults are filled, and local adjustments are made using drilling and well-logging data to refine the model and make it more representative of the actual conditions. Incorrect sharp points of interpretation are removed and reinterpreted. Multiple resampling and grid partitioning iterations are performed on the data points within the model to create a smooth representation of

FIGURE 3
Process of structural geological modeling and construction of fault–reservoir database.

the stratigraphic-fault system that captures curvature and segment trends. The stratigraphy is then connected to the simplified fault plane without thickness. Major faults like Cangdong Fault and Banqiao Fault are highlighted in red, while other secondary faults are marked in cyan. Different colors are used to indicate different periods of the basal stratigraphic layers. The process of grid partitioning and other steps is repeated iteratively until a visually appealing fault zone structural geological model is achieved within the region, indicating the completion of the initial modeling stage (Figure 4). Finally, relevant information on traps and reservoirs collected from published papers and scientific reports is digitized and imported into the model to establish a fault-controlled reservoir database. The reason for the fault plane being higher than the stratigraphic plane is that the latest stratigraphic boundary is currently represented by the Neogene Minghuazhen Formation. Above the Minghuazhen Formation, there are fourth-series rock layers, Holocene mud sediments, and overlying seawater.

4 Results

4.1 Ranking classification of faults based on structural geological modeling

The classification of fault levels in continental rift basins is typically conducted using seismic profile observations, a method widely employed in the Pearl River Mouth Basin and the Bohai Bay Basin in China (Song et al., 2018; Wang, 2020; Wu et al., 2019). In this study, we take the lower boundary of the Es1 member as an example. Based on seismic profile observations (Figure 5), combined with the development scale of faults in the three-dimensional model, the spatial distribution characteristics of faults (Figure 6A), contour maps of fault displacement (Figure 6B), the cross-cutting relationship of faults in seismic profiles, the thickness of hanging wall and footwall, the growth index, and the influence of faults on the development of internal blocks in the model (Chen et al., 2021), the fault levels in the Banqiao area can be classified into four categories.

The first-level faults include the Cangdong-Haihe Fault (Figures 5A, B; Figure 6), which is the largest fault in terms of scale and controls the basin boundaries. It has the greatest impact on the study
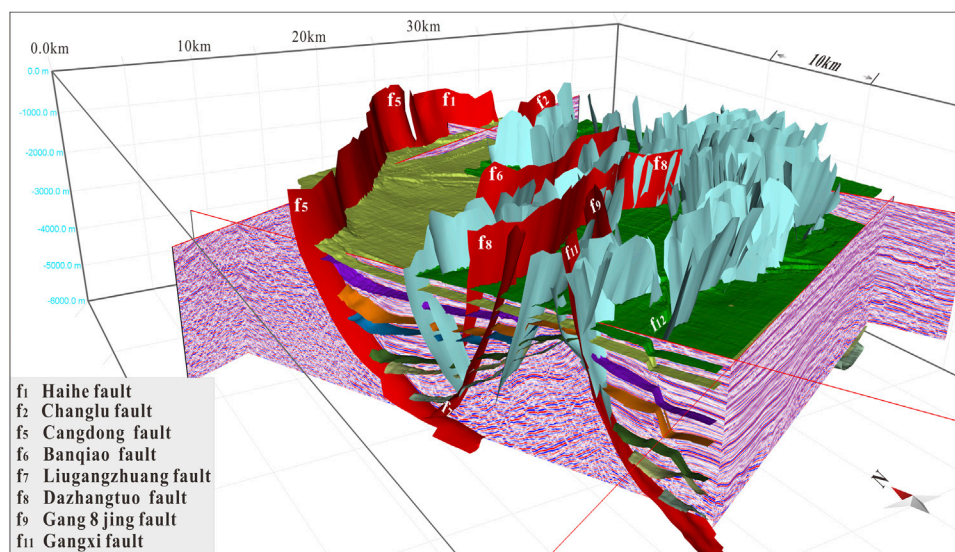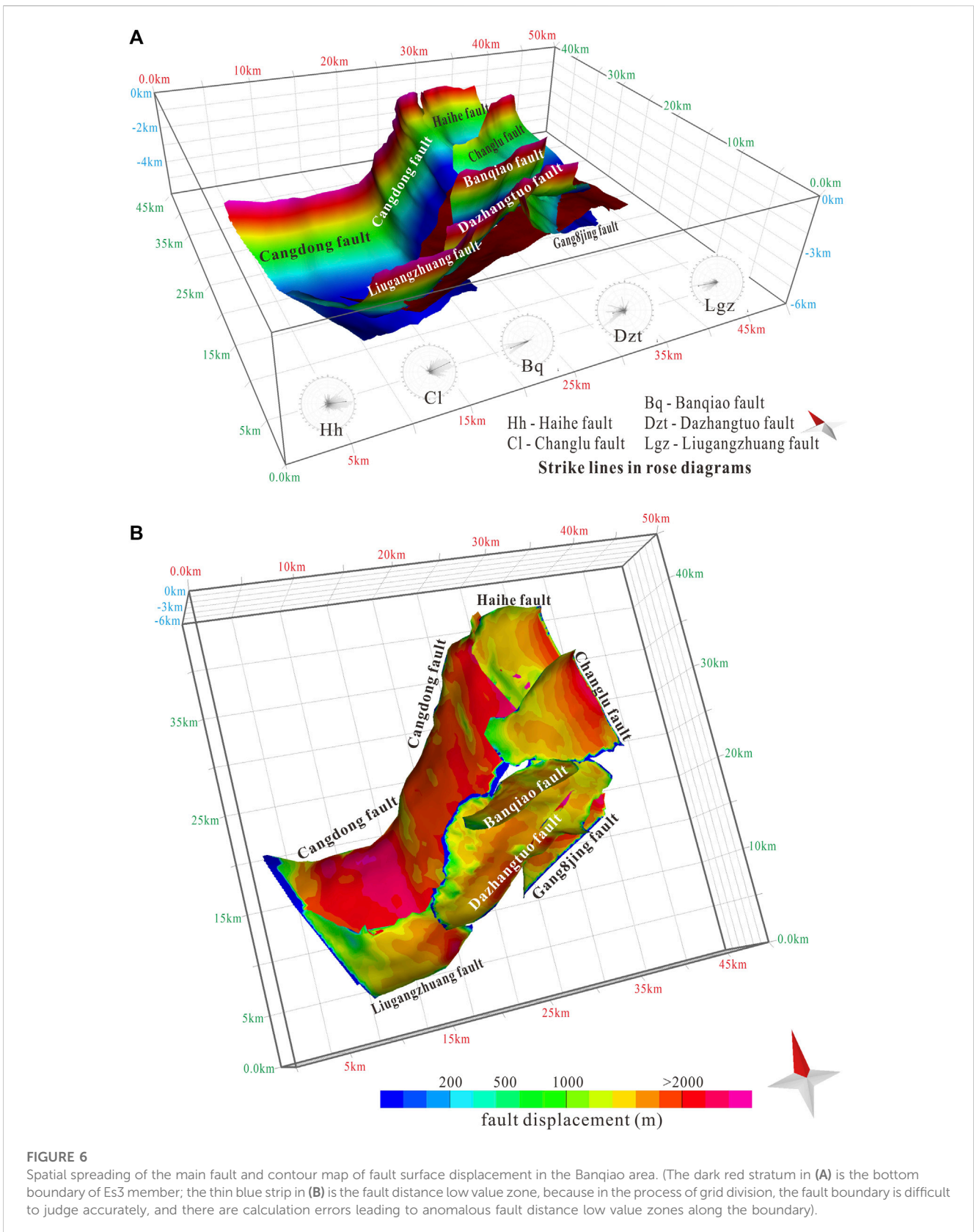
FIGURE 4
Schematic diagram of 3D structure modeling in Banqiao area.
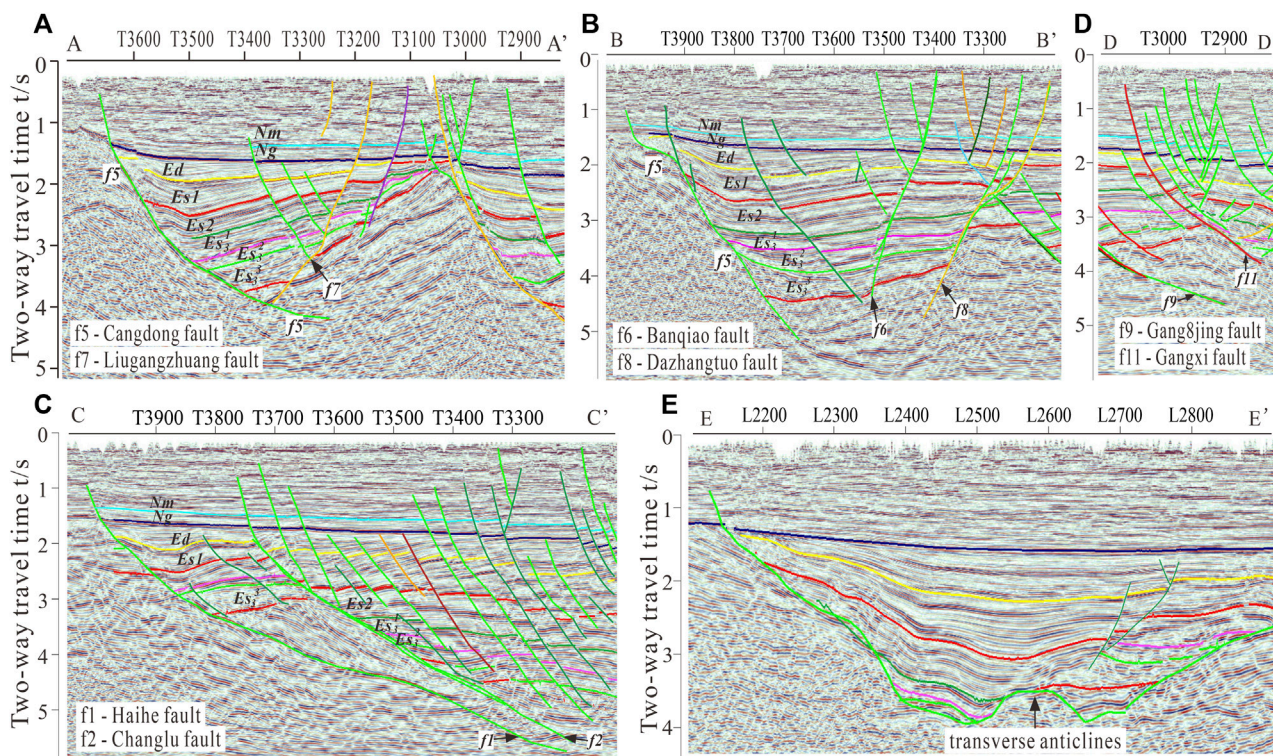
FIGURE 5
Seismic profile of the Banqiao area (the locations of these lines are located in Figure 1). In the southwest portion of the Banqiao area, there is a half-graben structural zone **(A)**; in the central area, a graben structural zone has developed **(B)**; in the northeast, there is an overlying, tile-like, shovel-shaped positive fault system **(C)**; The flower structure fault zone formed on the Gangxi fault **(D)**; Representative seismic profiles parallel to the structural trend are shown. Notice the distinct transverse anticlines in the bedrock base **(E)**.

area and is also referred to as the basin-controlling fault. The Cangdong Fault extends approximately 45 km in length in the Banqiao area, exhibiting significant cross-cutting characteristics.

Seismic profiles show that the Cangdong Fault cuts through the entire Cenozoic era, forming a steep upper segment and a gentle lower segment, presenting a shovel-shaped morphology. The

FIGURE 6
Spatial spreading of the main fault and contour map of fault surface displacement in the Banqiao area. (The dark red stratum in **(A)** is the bottom boundary of Es3 member; the thin blue strip in **(B)** is the fault distance low value zone, because in the process of grid division, the fault boundary is difficult to judge accurately, and there are calculation errors leading to anomalous fault distance low value zones along the boundary).

hanging wall of the Cangdong Fault mainly consists of strike-slip and reverse faults, cutting through the Es3 member and shallower units. As the boundary fault of the Banqiao area and even the Qikou

Depression, the Cangdong Fault exhibits distinct segmentation. The northern segment is approximately 30 km in length, trending NE and extending northward to the footwall of the Haihe Fault. The

southern segment is approximately 15 km in length, trending nearly EW. There are significant differences in the transverse structural profiles between the northern and southern segments. The Haihe Fault is a large-scale strike-slip fault developed in the hanging wall of the Cangdong Fault, and there is a tendency for a fault linkage at Line 2900. The Haihe Fault extends approximately 14 km within the Banqiao area, with a significant displacement and an approximate EW trend. The controlling influence of the Cangdong Fault diminishes towards the north and is replaced by the Haihe Fault, which controls the basin boundaries.

The Class II faults are boundary-controlling faults, including the Changlu Fault, Dazhangtuo Fault, Liugangzhuang Fault, and Gang8jing Fault (Figures 5A–C; Figure 6). These faults control the development of stratigraphy and the distribution of oil and gas in the area. Among them, the Dazhangtuo Fault is the most extensive, with the greatest displacement and the longest active period among Class II faults in the Banqiao area. It has a irregularly curved surface and extends approximately 25 km. The fault plane dips to the north, with a main trend of NNE. Within the central part of the depression, the Dazhangtuo Fault gradually develops into two segmented growth faults. One segment maintains its original trend and gradually fades away in the northeast direction, while the other segment trends east-west and connects with the Gang 8 jing Fault, which has an opposite trend. The spatial distribution of faults reveals a growth connection between the Liugangzhuang Fault and the Dazhangtuo Fault. The control effect of the Liugangzhuang Fault in the study area, from south to north, is gradually replaced by the Dazhangtuo Fault. The Changlu Fault is a large-scale, parallel fault located on the hanging wall of the Haihe Fault. Compared to other major faults within the study area, it has the smallest dip angle and trends NEE. It extends for approximately 15 km in the research area. The Haihe-Changlu Fault system jointly controls the formation of a southeastward imbricate thrust fault system in the study area.

The Class III faults are subsidiary major faults, primarily represented by the Banqiao Fault (Figure 5B; Figure 6). These faults exhibit relatively smaller displacements and have weaker effects on sedimentation and stratigraphic control. They mainly influence local structural features and the local hydrocarbon-water relationship. The Banqiao Fault trends NEE and extends for approximately 13 km. It is located on the hanging wall of the Dazhangtuo Fault and shares the same trend. Based on previous studies on fault displacement-distance relationships and fault activity rates (Chen et al., 2021), along with the analysis of fault surface morphology and contour lines of fault displacement (Figure 6), it can be inferred that the Banqiao Fault has undergone segmented growth. The growth connection point is located in the middle part of the Banqiao Fault plane. Prior to the Es1 period, the Banqiao Fault consisted of two isolated, small-scale growing faults. During the Es1 period, these two isolated faults underwent segmented growth connection. In the Ed period, they were in a transitional stage of soft connection, and in the Ng period, they developed into a hard connection, eventually forming a new major fault.
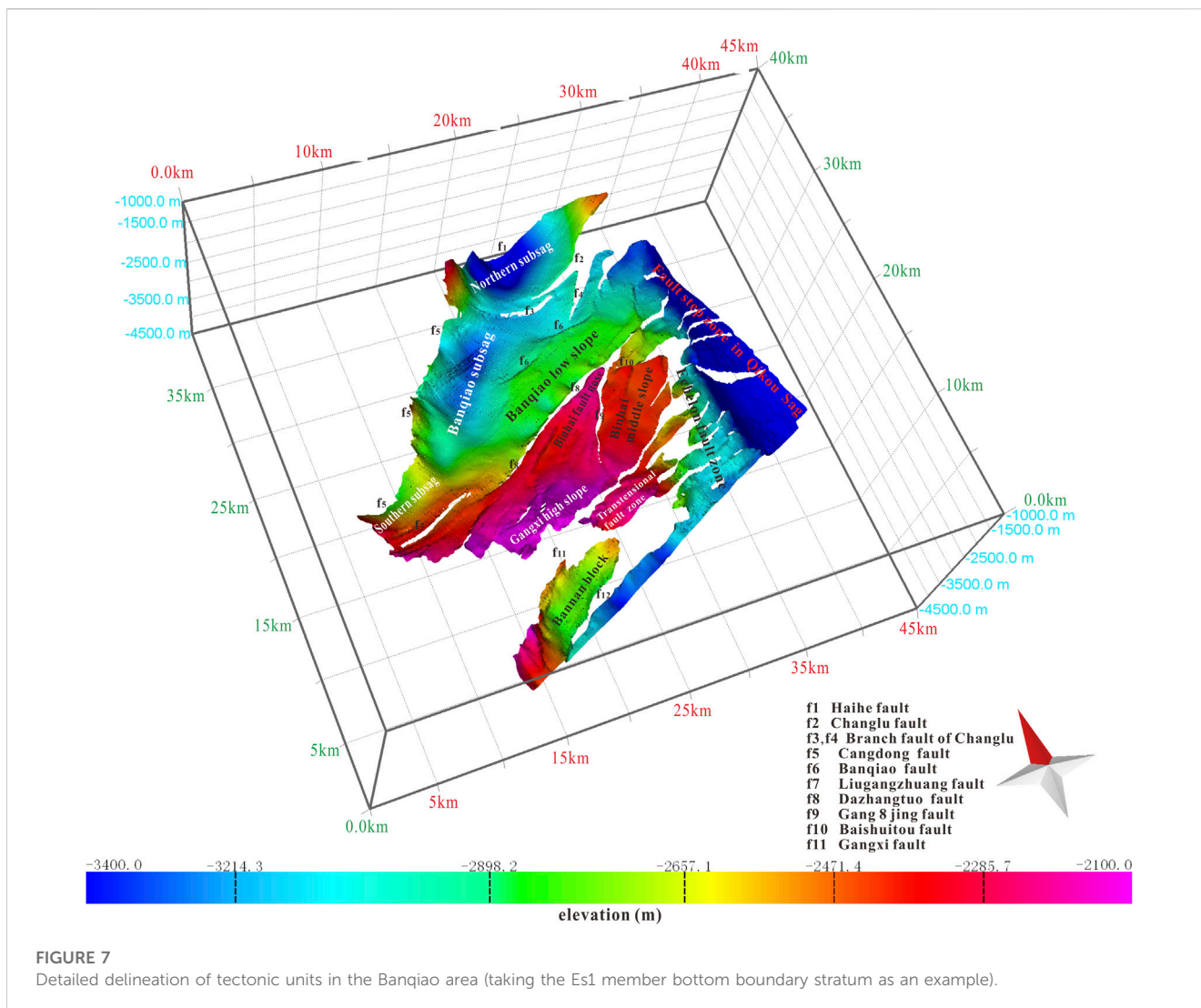
Class IV faults are secondary adjusting faults and can be classified into parallel subsidiary faults and antithetic adjusting faults. They generally exhibit smaller overall dimensions, with most of them extending no more than 7 km, typically ranging from 4 to 6 km. These faults are not coeval with sedimentation and possess relatively weaker cross-cutting characteristics. Most of them are unable to simultaneously penetrate multiple sets of strata and only adjust the local fault block structures. Based on previous studies on the tectonic evolution history (Chen et al., 2021) and the comprehensive analysis of fault displacements in this study, it can be inferred that the overall extensional strain in the entire study area is primarily influenced by Class I, II, and III faults, these faults play a dominant role in shaping sedimentation patterns and the distribution of geological strata, while Class IV and lower-level faults serve as auxiliary adjusting features.

4.2 Subdivision of tectonic units based on Structural Geological modeling

Based on the three-dimensional spatial distribution characteristics of the geological strata and faults, a refined subdivision of structural units can be conducted in the study area. Taking the Es1 member formation as an example, the study area can be divided into the subsag area, slope area, stress transition zone, fault step zone in Qikou sag, and Bannan block area (Figure 7). This subdivision allows for a detailed characterization and analysis of the different structural elements present in the study area, specifically within the Es1 member formation.

Based on the morphology of the stratigraphy and the response of faults, the subsag area can be divided into the northern subsag, the Banqiao subsag, and the southern subsag (Figure 7). The northern subsag covers an area of approximately 75 km^2 and is controlled by the Cangdong Fault, the Haihe Fault, the Changlu Fault, and the branch fault f3 of the Changlu Fault. It is located east of the Cangdong Fault, south of the Haihe Fault, and west of the Changlu Fault. The subsag has a greater burial depth, significant topographic relief, relatively fewer fault segments, and exhibits a tilted state in the stratigraphic layers. Clear extensional structures can be observed in cross-sections, and the overall shape of the depression appears as a spherical deep pit without a distinct long or short axis. The Banqiao subsag has a distribution area of approximately 100 km^2 and exhibits an ellipsoidal shape, with its long axis oriented in the NE direction. The cross-sections often show half-graben to graben morphologies, with the Cangdong Fault as the main controlling fault. The tilted strata in this subsag trend in the NW direction. The southern part of the Banqiao subsag is influenced by the reverse adjustment of the Dazhangtuo Fault, and extensional structures in the strata are prominent. The Banqiao Fault, developed in the northern part, accommodates some stress release and jointly controls the northern part of the Banqiao subsag with the Dazhangtuo Fault. Since the Es1 period, the Banqiao Fault and the Dazhangtuo Fault have undergone intense synchronous activity, resulting in predominantly near-horizontal strata between the surfaces of these two faults (Figure 5B; Figure 7). The southern subsag in the Banqiao area covers an approximate area of 20 km^2 and is primarily controlled by the Cangdong Fault and the Liugangzhuang Fault. Due to limitations in seismic data acquisition in the Banqiao area, the full extent of the Liugangzhuang Fault surface is not displayed (Figure 6), and only a partial morphology of the fault in the Banqiao area is shown. Utilizing previous data on the fault throw-distance curve and fault activity curve of the Liugangzhuang Fault (Chen et al., 2021), it is inferred that the overall shape of the southern subsag is elliptical, with its long axis trending in the NEE to nearly EW direction. The subsag
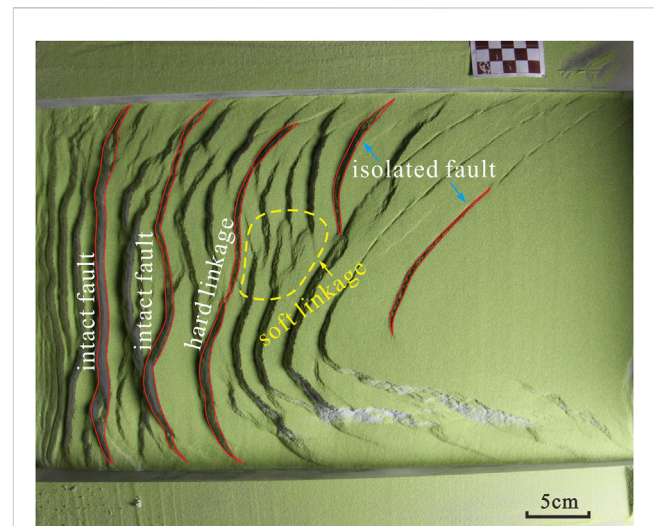
FIGURE 7
Detailed delineation of tectonic units in the Banqiao area (taking the Es1 member bottom boundary stratum as an example).

area extends over 50 km², and the boundary between the subsag and the Banqiao subsag is defined by the segmented growth connection of the Liugangzhuang Fault and the Dazhangtuo Fault. The subsag area exhibits a chain-like arrangement, gradually deepening from southwest to northeast, and has relatively fewer developed faults. This area has experienced minimal damage to hydrocarbon source rocks and is a favorable hydrocarbon generation zone in the Banqiao area.

The slope area includes Banqiao Low Slope, Binhai Middle Slope, Binhai Fault Nose, and Gangxi High Slope (Figure 7). The Es3 member in this area is characterized by the development of high-quality source rocks with high thermal maturity, providing a resource foundation for the formation of large to medium-sized natural gas fields. It is one of the main directions for breakthroughs in oil and gas exploration and increased reserves in the faulted basin. Banqiao Low Slope is an area sandwiched between the Banqiao Fault and the Dazhangtuo Fault. Seismic profiles show a gradual decrease in the dip angle of the Es3 member to the Es2 member. After removing the influence of traction and reverse traction from the overlying strata of the Dazhangtuo Fault, the strata have been nearly horizontal since the Es1 period without significant tilting. Since the Es1 period, the area between the two faults has

subsided synchronously in the form of blocks (Figure 5B). Binhai Fault Nose is located between the Dazhangtuo Fault and the Gang8jing Fault. The two faults form a ridge-like structure with opposite orientations. Seismic profiles exhibit features of faulted structures, deep-level strong throw, and shallow-level flower-like patterns. The fault nose is located near a branch of the broom-shaped fault system, which is a large-scale right-lateral en-echelon fault. The distribution and evolution of faults correspond well to the segmented characteristics of the Binhai Fault Nose structure. The Neogene tectonic features exhibit obvious zonation, and the internal fault activity in the fault nose is generally weak. The structural features inherit from bottom to top and develop as deep, large-scale, extensional nose-like structures under the background of ancient uplift. Binhai Middle Slope is located on the east side of the Binhai Fault Nose and is part of the fault nose in the Mesozoic. Since the Neogene, the regional extensional stress and the existence of a dextral strike-slip component have caused large-scale activity of the Gang8jing Fault, disrupting the original fault nose and developing into the present Binhai Middle Slope. Binhai Middle Slope is bounded by the Gang8jing Fault and is characterized by the development of a large number of south-dipping, parallel, imbricate normal fault

systems (Figure 4). Spatially, it exhibits a distribution of a densely fractured zone on a large scale, with most of the fault breaching the Shahejie Formation and a small portion breaching the Dongying Formation. Gangxi High Slope is located in the high point area of the Beidagang Qianshan Structural Zone, trending in a northeast direction. It is an uplift within the Qikou Depression and mainly consists of Middle Paleozoic and Mesozoic formations. Influenced by the faulting movement of the Qikou Depression, during the Es3 period, the Gangxi Uplift, located in the high point area of the Beidagang Qianshan Structural Zone, emerged and underwent uplift and erosion, becoming a stable provenance area. Although the Gangxi Uplift is not large in scale, with an Es1 member distribution area of approximately 50 km², it is an important source of detrital materials during the deposition period of the Shahejie Formation in the northern Gangbei and Qibei areas.

The stress transition zone in the Plate Bridge area refers to the change in stress direction that occurred during the rifting stages I (Es3 and Es2 periods) when the stress was oriented towards the northwest, and the transition took place during the rifting stage II (Es1 and Ed periods) when the extension direction shifted to a nearly south-north (SN) orientation. This extension continued until the post-rifting period. The "three-stage, two-direction" extensional deformation in the Plate Bridge area resulted in a dextral (right-lateral) strike-slip component, forming the stress transition zone (Chen et al., 2021; Liu, 2019; Liu, 2020). In the plan view, the stress transition zone exhibits right-lateral strike-slip fault blocks and a dextral echelon fault zone (Figure 7). The faults within this zone display non-coaxial extension, as observed in cross-sectional views with flower-like structures (Figure 5D). This zone includes the dextral echelon fault zone as well as the extensional-twist zone. Based on the relationship between the evolution of fault zones and multiple stages of extensional deformation, (Liu, 2020) classified oblique extension into four types: pure extension, extension-twist, twist-extension, and strike-slip, based on the angle between pre-existing faults and the regional extension direction. This classification was verified through structural sandbox physical modeling and applied to the Qikou Depression, demonstrating the existence of three types of densely fractured zones: pure extensional, extension-twist, and twist-extension. Similarly, the Banqiao area exhibits an extension-twist fault zone. The main boundary fault, the Gangxi Fault (NE-oriented), primarily experienced orthogonal extensional deformation during the Rift Phase I, resulting in predominantly dip-slip displacement. During the Rift Phase II and the subsequent sagging period, the fault zone displayed extension-strike-slip deformation. As the proportion of strike-slip displacement increased, strain primarily accumulated in the hanging-wall strata above the main controlling fault, forming flower-like structures on top of the Gangxi Fault (Figure 5D). Qu (2020) referred to this profile pattern as a tree-shaped flower-like structure. The coastal slope was also influenced by the strike-slip stress component, resulting in a right-lateral movement with the Gang8jing and Baishuitou faults serving as boundaries. The extension-twist structure is a type of detachment structure characterized by both strike-slip features and stretching deformation. It is the result of block rotation and uneven translation within a basin. The extension-twist structure is a product of strike-slip components reaching a certain level of
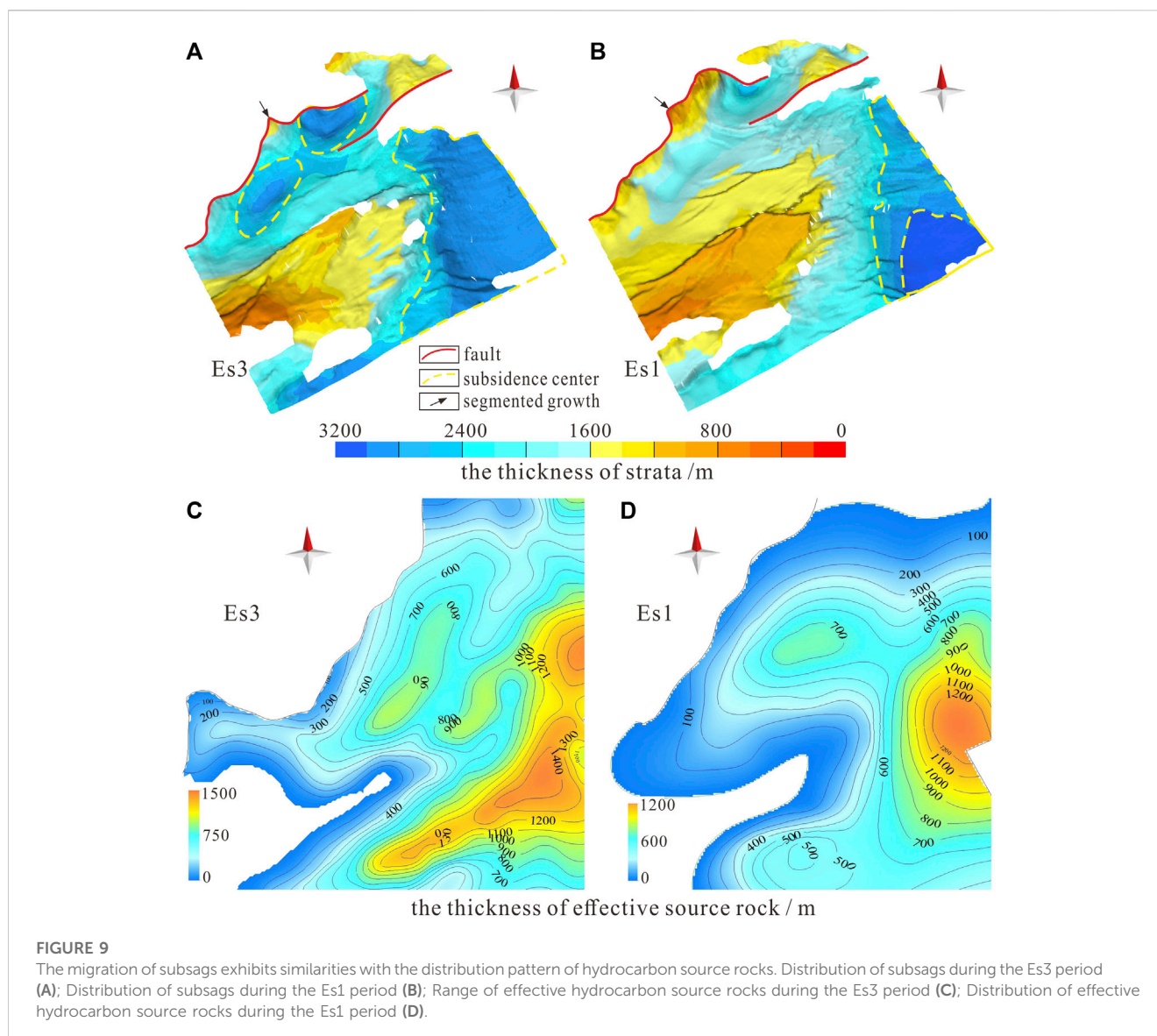

FIGURE 8
Sandbox simulation of fault segmentation growth connection (We can see how the fault grows from isolated to soft linkage, then to hard linkage, and finally becomes a complete intact fracture). (1) initially isolated faults can propagate toward each other; (2) fault segments (soft linkage) may interact without any obvious connections, and stress may be focused on the fault bridge (overlapping zone); and (3) as faults continue to slip (hard linkage), fault segments may evolve and link together by breaching the relay zone.

development in extensional basins and is widely present in basin tectonic systems. It controls the formation position, basin morphology, basin subsidence, sedimentation processes, tectonic deformation, and hydrocarbon accumulation in basins (Feng, 2015).

The Bannan block area refers to the block development located on the hanging wall of the Gangxi Fault. Its formation and evolution are mainly controlled by the Gangxi Fault and the F12 Fault, which act as the boundary faults. Based on seismic profiles (Figure 5A), there is evidence of detachment and sliding within the quasi-sedimentary basement, indicating the influence of inherited developmental processes. The footwall of the thrust fault remains relatively stable. It is speculated that there is a staircase-like block development south of the Banqiao area (Figure 7).

The fault step zone in Qikou sag refers to a deep depression located in the eastern part of the Banqiao area. It is characterized by the development of a roof-shaped imbricate thrust fault system, with the Haihe Fault as the main controlling boundary fault (Figure 7). The Haihe Fault and the Changlu Fault are the main faults in this region. Reverse faults that are opposed to the main faults gradually diminish within the area, and they are replaced by a significant development of coeval roof-shaped imbricate thrust faults. The internal faults of these thrust faults extend deep and can intersect with the main boundary fault, resembling a reverse fault with opposite displacement. The Haihe and Changlu Faults formed earliest, starting in the Es3 period. After the attenuation of processes such as tilting and compaction during the extensional phase, steep high-angle branching faults began to form. These combinations of faults create an upward fan-shaped structure known as a horsetail fault (Figure 5C).

FIGURE 9
The migration of subsags exhibits similarities with the distribution pattern of hydrocarbon source rocks. Distribution of subsags during the Es3 period **(A)**; Distribution of subsags during the Es1 period **(B)**; Range of effective hydrocarbon source rocks during the Es3 period **(C)**; Distribution of effective hydrocarbon source rocks during the Es1 period **(D)**.

5 Discussion

5.1 Formation and distribution of sags controlled by segmental growth of major boundary faults

Fault growth is a widespread phenomenon in the Earth's crust. The formation process of faults is similar to the deformation and failure of rigid bodies in material mechanics experiments. It can be understood as a sequence of events: intact rock layers experiencing stress, development of microscopic defects, formation of macroscopic cracks, expansion of these cracks, instability of the rock mass, initiation of small-scale fault segments, and further enlargement of fault scale. Fault segmentation applies not only to small microfractures but also to regional-scale major faults (Fossen, 2010). In fault growth, the generation of a single fault often involves multiple smaller faults. Fault segmentation is a ubiquitous process characterized by three distinct stages of evolution (Figure 8):

(1) initially isolated faults (stage 1) can propagate toward each other; (2) fault segments (soft linkage, stage 2) may interact without any obvious connections, and stress may be focused on the fault bridge (overlapping zone); and (3) as faults continue to slip (hard linkage, stage 3), fault segments may evolve and link together by breaching the relay zone (Conneally et al., 2014). Faults are commonly segmented at various scales (Fossen, 2016). As microfractures form, fractures grow, interact, and eventually coalesce into larger faults (Conneally et al., 2014; Fossen, 2016). Fault segmentation represents a transitional feature in the process of fault evolution, highlighting the essential role of interaction. The growth of fault segments is a dynamic process, and its quantitative characterization can address several key aspects: the migration of depocenters, determination of the location of variation zones to guide facies mapping, guidance for seismic interpretation to improve the quality of fault interpretation, identification of trap presence, analysis of trap-forming mechanisms, and determination of the timing of trap formation (Fu et al., 2015).

5.1.1 Formation and distribution of subsags controlled by segmental growth of major boundary faults with clear partitioning

The Cangdong Fault in the Banqiao area underwent segmental growth during the Es3 deposition period, dividing into approximately two connected segments delineated by the growth points shown in the figure. The southern segment of the fault exhibited greater activity and larger displacement during the Es3 period compared to the northern segment, and the two segments underwent segmental growth connection during the Es2 period (Figures 9A, B). Subsag migration is controlled by the segmented growth of the Cangdong Fault, resulting in a pattern with two subsag depocenters. During the Es3 period, the depocenters of the subsags in the Qikou sag were mainly controlled by northeast-trending faults, leading to a larger sedimentary area. In the Es1 period, the Banqiao slope area was influenced by inherited development, causing changes in subsidence within the northern and Qikou subsags, and their boundary became less distinct. They gradually merged into a larger depression, and the southern subsag also exhibited a noticeable decrease in size, with the subsidence center shifting northward and a thinning of sedimentary thickness. Transverse folds often form transverse synclines in the strongly concave parts of the fault plane and transverse anticlines in the strongly convex parts of the fault plane (McGill et al., 2000). Observations along seismic profiles parallel to the Cangdong Fault reveal distinct transverse anticlines in the development of the lower boundaries of the geological strata (Figure 5E). This is due to the relatively lesser activity of the fault at the segmented growth points, resulting in higher topography and the formation of anticlinal structures in that area. Wang and Liu (Liu, 2019; Wang, 2020) accurately inferred that the segmented growth connection of the Cangdong Fault occurred during the Es2 period using the maximum displacement subtraction method. They also calculated fault displacements for various geological periods and compared the thickness peak zones of the two ancient subsags during the Es3 period, which further confirmed the control of the segmented growth of the Cangdong Fault on the distribution of subsags.

5.1.2 The migration of subsags exhibits similarities with the distribution pattern of hydrocarbon source rocks

The formation of slope belts in the Qikou Depression is controlled by both basement subsidence and fault growth, leading to the development of multiple subsags that control the formation and evolution of high-quality hydrocarbon source rock (Liu, 2019). The Qikou center, Qibei, and Banqiao areas within the Qikou Depression exhibit the greatest overall subsidence, which is favorable for the development of hydrocarbon source rock. The Banqiao area also experiences significant tectonic subsidence, with the maximum subsidence exceeding 2,000 m in the low-slope region, indicating strong control by tectonic processes (Deng, 2018). During the Es3 deposition period, the Banqiao area exhibits overall strong fault activity, with the Cangdong Fault and the Binhai Fault having displacement rates of 600 m per million years (m/Ma) and the Dazhangtuo Fault exhibiting a rate of 150 m/Ma. Consequently, the Banqiao area undergoes overall subsidence. In the Es1 deposition period, the overall fault activity

weakens, with the Cangdong Fault and the Binhai Fault exhibiting reduced displacement rates of 300 m/Ma and the Dazhangtuo Fault exhibiting a rate of approximately 100 m/Ma. Additionally, the Banqiao Fault starts to become active with a rate of 20 m/Ma. The varying activity rates of these faults lead to changes in the slope morphology, resulting in tilting and overturning of the slope belts, and the subsidence centers shift towards the northeast (Wang, 2021).

Various factors, including the thickness, distribution, and hydrocarbon generation potential of source rocks, play a pivotal role in determining the size and reserves of oil and gas reservoirs (Wang, 2021). Due to variations in accumulation, the Banqiao area exhibits significant disparities in the distribution of oil and gas. These differences are not only noticeable between different oil-bearing strata but also within distinct structural locations within the same strata. Oil and gas resources are predominantly concentrated in two primary hydrocarbon generation centers: the Banqiao trough and the Qikou main depression. Most hydrocarbons are notably abundant in the Binhai middle slope, Binhai fault nose, Gangxi high slope, and the stress transition zone (Figures 9C, D). Limited displays of oil and gas are also observed in the Banqiao subsag within the trough. The distribution of oil and gas gradually expands from the Es3 to the Es1x strata and then drastically contracts starting from the Es1z strata. The distribution of source rocks in the Banqiao area is strongly influenced by the evolution of the Cangdong Fault and the underlying structure of the Qikou Depression. The primary center of source rock distribution is situated in the Qikou main depression, owing to the fact that the sedimentary depocenter was originally located within this depression prior to the Neogene era. The Cangdong Fault gradually transformed into a boundary fault during the Neogene period, resulting in the emergence of two prominent source rock thickness centers within the study area.

A comprehensive comparative analysis of effective source rocks in the Banqiao area of the Bohai Bay Basin reveals that the primary hydrocarbon source rock sequences, from bottom to top, consist of the Es3 and Es1x source rock layers (Deng, 2018). These layers predominantly comprise black and gray-black mudstone, with the Es3 source rock layer exhibiting the maximum thickness, widest distribution, and a distinct belt-like distribution pattern. The primary center of source rock thickness is primarily located within the Qikou main depression, exceeding 1,000 m in thickness and gradually thinning towards the surrounding areas. A secondary thickness center is identified within the Banqiao trough, displaying an elliptical distribution trending northeastward.

During the Es3 to Es1x period, the intensity of fault activity in the Banqiao Fault, Dazhangtuo Fault, Gang 8 Well Fault, Baishuitou Fault, and the major fault near the interior of the Qikou main depression was considerably lower than that of the controlling fault, namely, the Cangdong Fault. This reduced influence of the controlling fault led to a relatively limited supply of source materials near these faults, thereby creating favorable conditions for the accumulation of organic-rich mudstone and the development of source rocks in a reducing environment. In the Es1z to Ed period, the activity of the aforementioned faults intensified, resulting in rapid subsidence within the depression. However, the coarse grain size of the clastic materials supplied was unfavorable for the formation of regional source rocks. Simultaneously, the increased
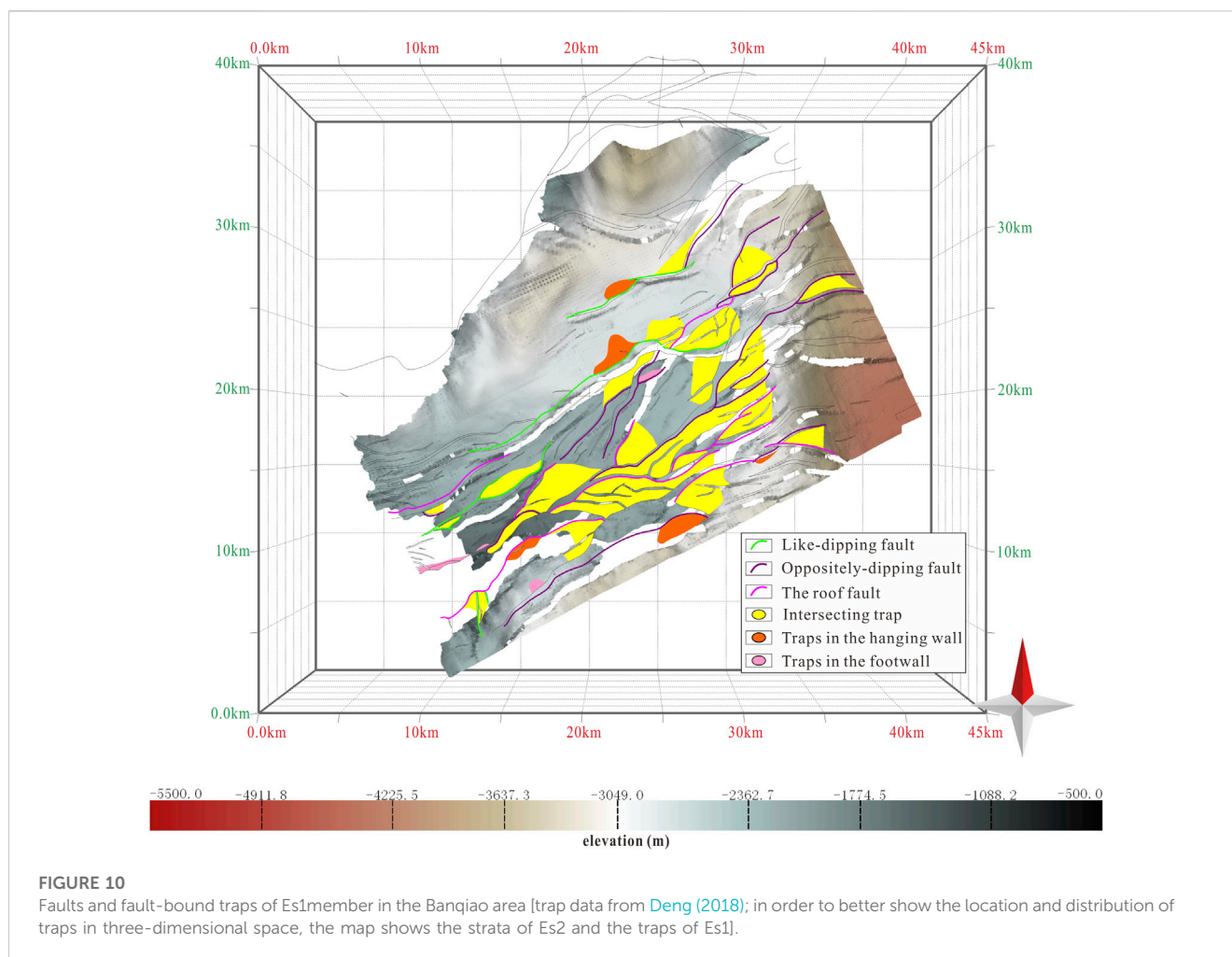
FIGURE 10
Faults and fault-bound traps of Es1member in the Banqiao area [trap data from Deng (2018); in order to better show the location and distribution of traps in three-dimensional space, the map shows the strata of Es2 and the traps of Es1].
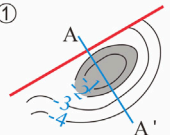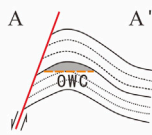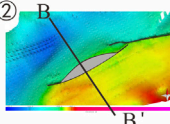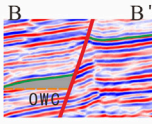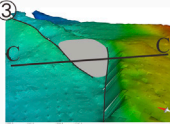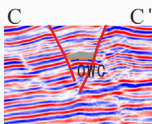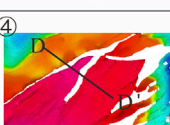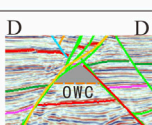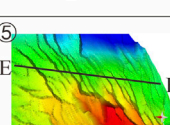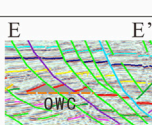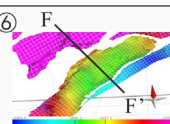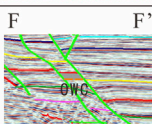
fault activity rate accelerated the burial and thermal evolution of the Es3 and Es1x source rocks.

In the northwestern part of the Banqiao area, under the influence of the activity of the Cangdong Fault and the basin's structural control, the migration of the subsidence centers occurs continuously (Ma et al., 2010). Based on the distribution of subsags and sedimentation centers in the Qikou area during the Es3 and Es1 periods (Figure 9), combined with Deng's research on the distribution of high-quality source rocks and effective source rocks (Deng, 2018), it can be observed that the development characteristics of effective source rocks exhibit similar patterns under the control of the continuous eastward migration and shrinking background of subsidence centers. Comparing the distribution characteristics of effective source rocks (TOC > 0.5, Ro > 0.5%) during the Es3 period with those during the Es1 period in the Qikou area (TOC, total organic carbon; Ro, the organic maturity), it is evident that the sedimentation centers in the area significantly shrink and migrate eastward from the Es3 to the Es1 period. The range of source rock development gradually decreases, resulting in thinner thickness. As a result, the distribution range of effective source rocks during the Es1 period in the southern sub-depression of the Banqiao slope significantly reduces. The development characteristics and variations of high-quality source rocks (TOC > 2) exhibit a similar pattern.

In conclusion, the fault activity in the Banqiao area has created accommodation space within its subsiding block, determining the lateral extent and vertical thickness of sedimentary deposits. This activity has also driven the migration of subsiding troughs, ultimately influencing the accumulation of source rocks within the basin.

5.2 Matching relationship between fault system and trap in the Banqiao area

The traps formed by fault blockage are known as fault-bound traps, which are a typical type of structural trap formed during periods of fault activity. Oil and gas in fault-bound traps are sealed by faults, preventing lateral migration (Chu, 2019; Fu et al., 2021; Liu, 2019). There are three main mechanisms for the formation of fault-bound traps: shale smear, grain fragmentation, and diagenetic sealing (Fu et al., 2012a). There are various classification methods for fault-bound traps, including classification based on fault type, displacement, morphology, relative position, etc. Common types include normal fault traps, reverse fault traps, strike-slip fault traps, block fault traps, and fault-related traps. These types of traps are widely distributed worldwide, particularly in areas with frequent tectonic activities, such as the California Basin in North America, the

FIGURE 11
Types of fault-bound traps and the role of faults in hydrocarbon accumulation in Banqiao area (OWC, Oil Water Contact).

North Sea Basin in Europe, the Niger Delta Basin in Africa, and the Bohai Bay Basin in China (Liu, 2019). The Bohai Bay Basin, a continental rifted sag basin in China, has developed numerous fault-bound traps. The formation of fault-bound traps in this basin is closely related to geological tectonic activities. Different mechanisms of fault formation, fault growth processes, and the relationship between faults and sand body configuration can result in different types of fault-bound traps (Fu et al., 2021; Liu, 2019).

5.2.1 Classification of fault-bound trap in the Banqiao area

The trap formation in the Banqiao area occurred early, prior to the main hydrocarbon expulsion period of the source rocks, providing favorable conditions for the accumulation and preservation of oil and gas resources (Deng, 2018). The filling and tectonic evolution characteristics of the rift basin have resulted in the formation of various types of traps, with structural traps being predominant. In addition to structural traps, sandstone pinch-out traps and stratigraphic overlap traps have developed at the local margin of the depression, while isolated sand body traps are present in the central depression. The Banqiao area has a complex internal fault system due to ongoing tectonic

movements. Oil and gas reservoirs are distributed along faults due to the vertical and lateral sealing effects of the faults, with fault-bound traps being the dominant type of structural traps. By summarizing the existing literature and relevant data on the Banqiao area (Deng, 2018; Liu, 2019; Wang, 2020) and digitizing the trap configurations within the study area, quantitative or semi-quantitative evaluations of fault-bound traps can be conducted using modeling techniques (Figure 10). Based on the boundaries formed by faults in trap formations (Chu, 2019; Liu, 2020; Wang, 2020), fault-bound traps can be classified into self-contained traps and fault-bounded traps, which can be further subdivided into the following modes (Figure 11):

Single-fault-controlled trap mode: This mode refers to the fault-bounded traps formed by the southern segment of the Banqiao Fault during its evolutionary process. The Banqiao Fault acts as the trapping boundary, primarily obstructing the migration of oil and gas. It is speculated that the Banqiao Fault has a strong sealing capacity (Figure 11②).

Intersecting faults controlled trap mode: there is an oblique intersection between the southern branch of the Changlu Fault and the northern segment of the Banqiao Fault. The model cross-section indicates fluid trapping within V-shaped fault blocks, which is a

commonly observed type of fault-bound trap in the Banqiao area (Figure 11③). Another example is the interaction between the northern segment of the Dazhangtuo Fault and the Gang8jing fault. These two faults have opposite orientations, and fluid trapping occurs within A-shaped fault blocks (Figure 11④).

Leteral-faults-controlled trap mode: This mode consists of multiple faults with the same orientation that are unable to intersect but instead form an overlapping and inclined system of en echelon normal faults. These faults jointly control fluid migration and primarily act as barriers. Based on existing data, this type of fault-bound trap is developed on a large scale in the dextral Yanlie Belt and the Qikou main depression fault step (Figure 11⑤).

Multiple faults controlled sealing trap mode: This mode involves multiple faults interacting to form complex fault blocks. The faults act as trapping boundaries, with obstruction being the primary effect and channeling being secondary. This type of trap is developed in the transpressional-tensional fault zones (Figure 11⑥).

By combining structural geological modeling, it is observed that the study area predominantly exhibits fault-bound traps controlled by intersecting faults (Figure 4; Figure 11).

5.2.2 Segmental growth of faults controls the spatial configuration of fault-bound traps

In the field of tectonic deformation research, the classification of faults into "like-dipping" and "oppositely-dipping" faults, based on Peacock's approach, is commonly used (Peacock, 2000). In this classification, faults that have a similar dip direction as the main fault within a local area are referred to as "like-dipping" faults, while those with a different dip direction are referred to as "oppositely-dipping" faults. On the other hand, in the context of fault trapping and fault seal analysis, Cloos' classification is often employed, where faults with the same dip direction as the bedding planes are called "like-dipping" faults (also known as parallel faults), while those with a different dip direction are termed "oppositely-dipping" faults (Cloos, 1928). Given that this study focuses on fault trapping and fault-controlled hydrocarbon accumulation, the second concept is adopted. Along the BB' traverse, which crosses the Plate Bridge fault, the fault orientation aligns with the bedding planes, resulting in a "like-dipping" fault-bound trap (Figure 11②). Similarly, in the region of the echelon faults zone, the EE' traverse exhibits "oppositely-dipping" fault-bound traps (Figure 11⑤).

Fossen proposed the concept of fault segmentation in macroscopic scales, mesoscale rock samples, and microstructural analysis (Fossen, 2016). Field outcrops and 3D seismic data have also confirmed the process of fault segmentation (Chen, 2019; Reeve et al., 2015). Laboratory experiments using structural sandbox simulations further demonstrate the process of fault segmentation: during the isolated nucleation stage, multiple individual fault planes are formed; in the soft linkage stage, fault planes are not completely overlapping, resulting in a series of transitional ramps; in the hard linkage stage, two or more fault planes exhibit similar orientations and inclinations, showing partial overlap and development of parallel fault-related folds; when there is significant overlap and a common trend among the fault planes, a new complete major fault phase is established (Figure 9). Based on

seismic data interpretation of fault structures, the board-bridge fault is characterized by the overlap of two thrust surfaces, which can be observed as connected arcs when viewed from a top-down perspective, indicating clear segmentation (Figures 4, 6, 7, 13②). Displacement-distance and fault activity rate curves provide further evidence of the segmented growth nature of the board-bridge fault (Chen, 2019; Chen et al., 2021).

Fault segmentation can control the spatial relationships of fault-bound traps through various mechanisms. One way is through the development of fault-related folds, where the bending of fault planes due to changes in fault movement direction or geometric variations of fault zones can generate fault-related folds. Fault segmentation can result in the development of multiple fault-related folds along the fault zone, leading to the formation of uplifted blocks and subsided basins that facilitate the accumulation of subsurface fluids. Additionally, fault segmentation can control the juxtaposition of different lithologies such as sandstones and shales, imparting distinct porosity and permeability characteristics, making them potential reservoirs for oil and gas accumulation (Fu et al., 2012b; Fu et al., 2015; Fu et al., 2012a).

Like-dipping fault-bound traps typically exhibit transverse anticlines of varying amplitudes. This is because, in cross-sectional profiles along the fault strike, the traps are often located at higher elevations of the anticlines, coinciding with the segment boundaries of the fault's segmentation. Due to the larger throw in the central portion and smaller throw at the ends of a normal fault, the segments of the fault tend to occur at the fault ends. Consequently, when the hanging wall of the fault undergoes downward displacement, the strongest vertical deformation occurs in the portion with the largest throw, while the portion with a relatively smaller throw experiences less vertical movement. This results in the higher elevation of the fault segment with a smaller throw, forming an anticline.

Oppositely-dipping fault-bound traps (Figure 11⑤), refer to traps formed under the control of reverse faults. Unlike like-dipping fault-bound traps, these traps typically form on the side of the slope closer to the trough. For a reverse fault, the hanging wall is on the side closer to the trough, and during the activity of a reverse fault, the hanging wall experiences relative uplift while the footwall undergoes relative subsidence. At the segment boundaries of the fault's segmentation, the hanging wall experiences less vertical movement in areas with smaller throws, whereas areas with higher throw values exhibit more significant vertical uplift. This elevation difference leads to the formation of the trap.

Intersecting fault-bound traps, as the name implies, form primarily due to the intersection of multiple faults, which collectively control the formation of the trap. These traps are often controlled by the intersection of two faults, but they can also involve multiple intersecting faults. Moreover, the controlling faults can be either of the same dip direction (Figure 11⑥) or of opposite dip directions. Typically, inactive fault segments intersect with long-term active fault segments, providing both migration pathways and lateral sealing properties. The boundaries of these traps are usually defined by fault segments, and the formation of intersecting fault-bound traps is primarily attributed to multiple episodes of oblique extension and superimposed deformation (Morley et al., 2007).
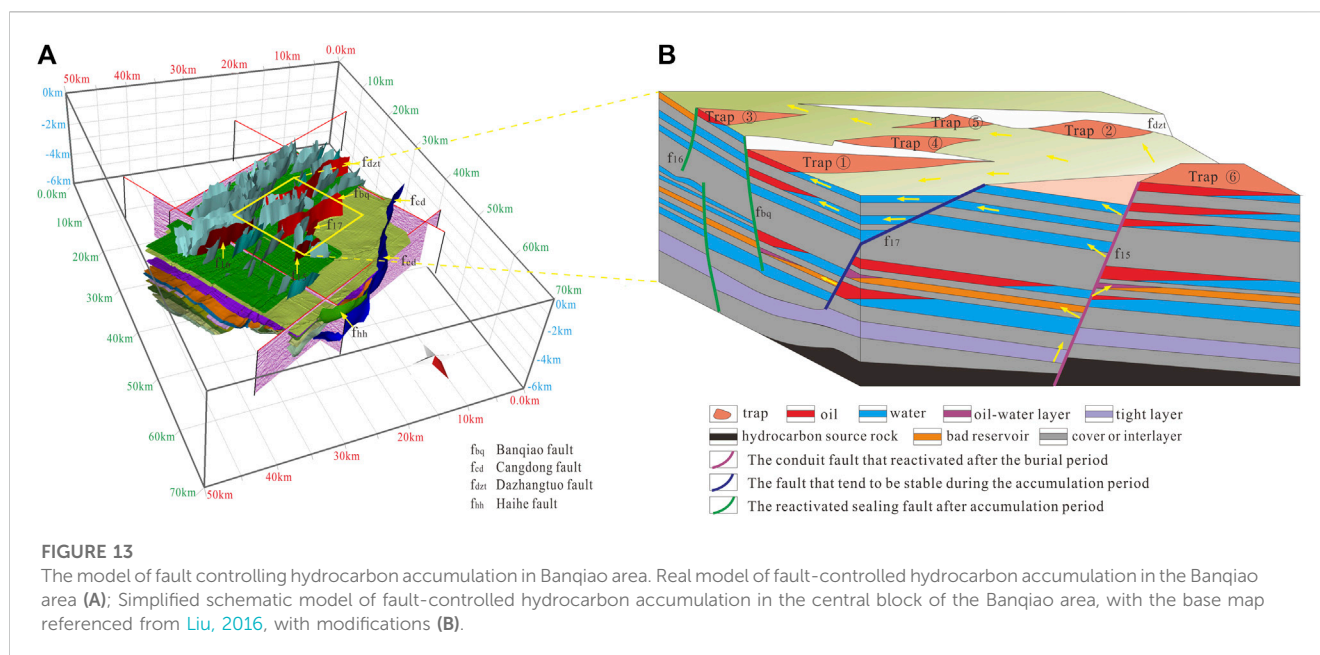
FIGURE 12
Fault system division (example of Es1 sections) (Chen et al., 2021).
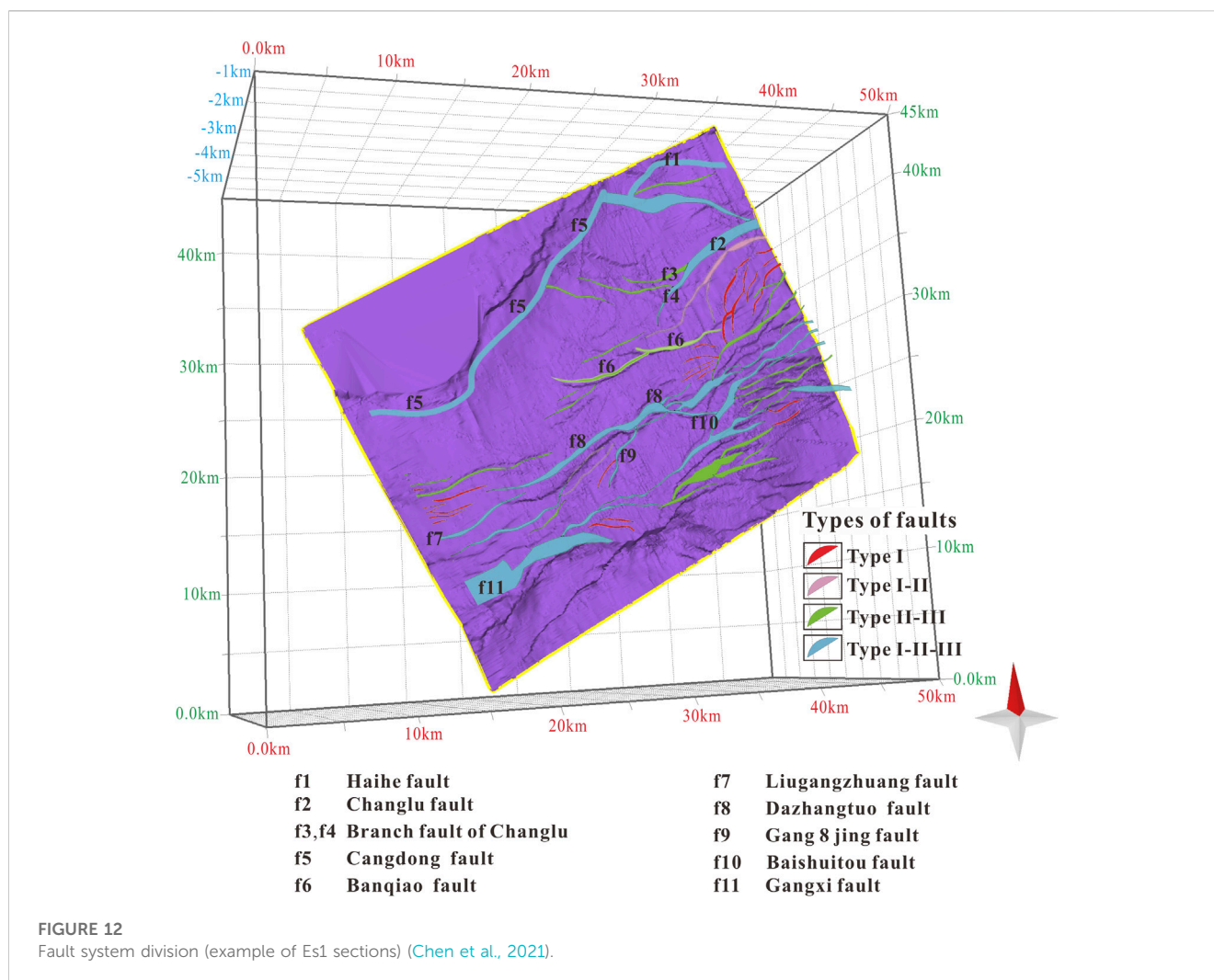
5.3 Fault-controlled hydrocarbon accumulation model in Banqiao area

The theory of fault-controlled hydrocarbon accumulation encompasses the concepts of fault control over basin formation, sand deposition, reservoir development, migration pathways, and preservation of hydrocarbons (Fu et al., 2015; Liu, 2019). The fault-controlled hydrocarbon accumulation models in rifted lacustrine basins can be classified based on various factors, such as the differential evolution of fault-dense zones (Liu, 2020), internal structure of fault zones (Jiang et al., 2016), establishment of fault information databases (Wu et al., 2019), characteristics of fault reactivation and evolution (Xie et al., 2015), and timing of fault activity and sealing layers (Peng et al., 2016). Regarding the classification of fault-controlled hydrocarbon accumulation models in the Banqiao area, Song et al. categorized the reservoir control patterns into two types based on factors such as fault scale. The first type is the "concomitant control of shallow and deep faults" model, primarily controlled by second-level faults like Dazhangtuo Fault. The second type is the "secondary fault-associated shallow control" model, controlled by third-level and fourth-level faults within the faulted basin (Song et al., 2016). Han et al. (2020),

considering trap types, distribution of sedimentary sand bodies, timing of hydrocarbon charging, and periods of fault activity, classified the fault-controlled hydrocarbon accumulation models into three types. These include the inheritance model of fault-controlled hydrocarbon accumulation controlled by faults like Dazhangtuo Fault, the early decline model of fault-controlled hydrocarbon accumulation controlled by the Changlu Fault system, and the late-stage model of fault-controlled hydrocarbon accumulation controlled by small-scale secondary faults.

Based on factors such as the activity phases of faults within the Banqiao slope and the tectonic evolution of the working area, the fault system in the study area is classified into six types: Rift Phase I faults (Type I), Rift Phase II faults (Type II), post-rift faults (Type III), Es-Ed period faults (Types I-II), Es1-Ed-Ng-Nm faults (Types II-III), and Es-Ed-Nm faults (Types I-II-III) (Figure 12) (Chen et al., 2021). Type I faults are characterized by fault activity only during Rift Phase I, followed by a period of quiescence. These faults are predominantly concentrated in the northeastern part of the Banqiao area along the Qikou Depression Fault Belt, developed in the Es3 and Es2 strata. They exhibit predominantly planar fault surfaces, indicating localized brittle deformation. Their orientations are consistent with the surrounding major faults,

FIGURE 13
The model of fault controlling hydrocarbon accumulation in Banqiao area. Real model of fault-controlled hydrocarbon accumulation in the Banqiao area **(A)**; Simplified schematic model of fault-controlled hydrocarbon accumulation in the central block of the Banqiao area, with the base map referenced from Liu, 2016, with modifications **(B)**.

and they are relatively small in scale, typically intersecting only one or two sets of strata, suggesting that the local stress field near Type I faults following the Rift Phase I is relatively weak and insufficient to reactivate the faults. Type II faults refer to faults that exhibit activity only during Rift Phase II and cease activity during the post-rift period. Some of these faults only intersect the Es1-Ed section, exhibiting small dimensions, and are adjacent to major faults with similar orientations. They predominantly exhibit planar fault surfaces. Another set of Type II faults, larger in scale and with stronger fault penetration, can traverse both the Shahejie Formation and Dongying Formation, exhibiting shovel-shaped fault surfaces. These faults are developed in the central and northeastern parts of the Banqiao slope. Type III faults are faults that developed only during the post-rift period and are extensively distributed in the Banqiao slope. They intersect the Ng-Nm or higher stratigraphic units. They vary in scale, with smaller faults developed only in the Ng or Nm strata, while larger faults can extend to the surface, forming "through-going faults." A few individual faults may extend downward to the Es1 strata, but they have limited control over the sedimentation of the strata. Type I-II faults indicate that the faults were active during Rift Phases I and II, followed by a period of quiescence. These faults are often larger in scale, with a wide spatial distribution throughout the entire area. The faulted strata are predominantly concentrated in the Es and Ed periods, with some individual faults extending upward into the Ng strata, but they have limited control over sedimentation. Type II-III faults indicate that the faults have been active from the Es1 period of Rift Phase II to the Ng-Nm period. These faults exhibit strong activity and significant fault penetration, with some individual faults traversing the entire set of Cenozoic strata and exerting control over sedimentation. They have a wide spatial distribution, and the Banqiao Fault is an example of this type of fault. One branch of the Changlu Fault, labeled f3, also belongs to this type of fault and is more developed in the northeastern part of the Banqiao area, while

less developed in the southwestern part. This type includes a fault in the northern part of Liugangzhuang and a branch fault of the Binhai Fault System. Type I-II-III faults indicate that the faults have been continuously active during both the Paleogene and Neogene, without periods of quiescence. This category includes faults such as Dazhangtuo, Liugangzhuang, Haihe, and Changlu faults, as well as the shovel-shaped boundary faults controlling sedimentation in the working area, such as the Cangdong Fault. These faults are characterized by their large scale, extensive spatial distribution, long strike length, and significant fault penetration. They can traverse the entire sequence of Paleogene and Neogene strata. These faults are considered the main faults in the study area and play a crucial role in the formation and evolution of the Banqiao slope, as well as the development of secondary faults.

The Banqiao area belongs to a rifted and subsided basin, where faults play a crucial role in the process of hydrocarbon accumulation. Based on the classification of fault systems (Chen et al., 2021), typical hydrocarbon reservoirs are dissected, taking into account the comparison of hydrocarbon sources and the results of the hydrocarbon generation and accumulation periods (Deng, 2018). Two types of fault-controlled reservoirs can be identified in the Banqiao area: source faults and barrier faults. Source faults refer to a type of fault system that was active during the critical period of hydrocarbon accumulation, providing pathways between source rocks and reservoirs, such as the Dazhangtuo Fault. Barrier faults, on the other hand, are inactive during the critical period but act as lateral barriers, contributing to the formation of hydrocarbon accumulations, such as the Banqiao Fault (Figure 13). In the evaluation of complex fault-block hydrocarbon reservoirs in rifted basins, different aspects of these two types of fault-controlled reservoirs are emphasized. For source faults, the focus is primarily on their vertical pathways for hydrocarbon migration during the accumulation period. For barrier faults, the evaluation mainly considers their lateral sealing

capacity, including the height of the hydrocarbon column they can seal and the degree of hydrocarbon enrichment (Fu et al., 2012a).

Based on the tectonic geological characteristics, fault system classification, and the geological model database of fault-reservoir relationships in the Banqiao area, this study identifies four fault-controlled hydrocarbon accumulation models (Figure 13).

1. Like-Dipping Fault-Controlled Model: This model involves the formation of fault segments with same-dipping faults due to differential fault activity. The hanging wall closure of these fault segments provides trapping conditions for hydrocarbon accumulation. Hydrocarbons mainly accumulate in the Paleogene reservoirs, controlled by Type I, Type II, and Type I-II faults. During the hydrocarbon accumulation period, the faults are inactive and act as hydrocarbon traps (Figure 13, Trap 1 and Trap 2). Well data from multiple drilling sites in the central part of the Banqiao area show that the reservoirs controlled by like-dipping faults exhibit both single-layer and multi-layer hydrocarbon-bearing characteristics (hydrocarbons controlled by like-dipping faults such as Banqiao and Dazhangtuo are distributed in the Es2, Es1, and Ed formations). In contrast, wells controlled by "Oppositely-dipping" faults (f16) typically exhibit single-layer hydrocarbon occurrences. The development of faults in the Banqiao area shows evident inheritance, with the late Nm deposition period being the main hydrocarbon accumulation phase in the area (Deng, 2018). Faults that were active during this period can vertically adjust the lateral migration of hydrocarbons. In the central part of the Banqiao area, hydrocarbons are mainly accumulated in the hanging walls of the Banqiao fault (Figure 13, trap①) and the Dazhangtuo fault (Figure 13, Trap②).

2. Oppositely-Dipping Fault-Controlled Model: This model involves the formation of fault nose structures between two or more fault segments beneath oppositely-dipping faults. The f16 fault in the Banqiao area cuts through mainly sandy-muddy interbedded strata of the Paleogene. Instead of rigid displacement, the fault forms a smeared fault core composed of mudstone, preventing direct sandstone-to-sandstone juxtaposition across the fault. This creates closure capacity, which is enhanced by subsequent burial compaction during late-stage sediment filling. The f16 fault acts as a barrier, providing trapping conditions for hydrocarbon accumulation. The main hydrocarbon accumulation period occurs in the Es interval, controlled by Type I, Type II, and Type I-II faults that are inactive during the hydrocarbon accumulation period (Figure 13, Trap 3). The probability of hydrocarbon accumulation in fault blocks controlled by oppositely-dipping faults is higher than that in blocks controlled by like-dipping faults.

3. Intersecting Fault-Controlled Model: This model occurs during oblique extension, where torsional and gravitational stresses cause segment growth with fault displacement and misalignment. The displacement and offset of intersecting faults create effective reservoir space. Shear forces from relative movement deform the strata within the trap, forming various hydrocarbon reservoir spaces. The relative movement also generates complex fracture and pore systems within the rock

layers, providing trapping conditions for hydrocarbon accumulation. Hydrocarbons in the intersecting fault traps primarily accumulate during the intense faulting phase in the Es3 and Es2 intervals. The trapping is controlled by Type I, Type II, and Type I-II faults, which are inactive during the hydrocarbon accumulation period. The fault blocks are formed by the juxtaposition and intersection of two or more stratigraphic units, with the footwall ascending and covered by the hanging wall, creating a sealed box-like structure that prevents fluid migration upward or downward, thus forming the intersecting fault-controlled hydrocarbon reservoirs (Figure 13, Trap 4 and Trap 5).

4. Reactivated Fault-Controlled Secondary Hydrocarbon Accumulation Model: Under the reactivation of faults, the surrounding rock masses undergo deformation and fragmentation, expanding existing pores and fractures and generating a series of new ones. These openings provide storage and migration pathways for hydrocarbons, increasing the storage capacity and improving reservoir properties, resulting in secondary hydrocarbon accumulation. Secondary hydrocarbons mainly accumulate in the Es1 and Ng intervals. After the hydrocarbon accumulation period, continued tectonic changes cause fault reactivation, disrupting early-formed hydrocarbon accumulations. Hydrocarbons migrate upward along the reactivated faults, forming shallow secondary oil reservoirs. The fault system controlling these reservoirs is the Type I-II-III fault system (Figure 13, trap⑥).

6 Conclusion

The Banqiao area exhibits multiple phases of oblique extensional deformation, resulting in the development of complex faulted oil and gas reservoirs of various types. Faults play a crucial role in basin formation, hydrocarbon generation, and reservoir accumulation. This study, based on structural geological modeling and the establishment of a fault-reservoir database, draws the following conclusions:

The Banqiao area can be categorized into four fault levels and five structural units. The segmented growth of faults regulates the formation and evolution of subsags, and there is a notable resemblance between the migration of subsags and the distribution patterns of source rocks.

Fault-related traps in the Banqiao area can be classified into two types: single-fault-controlled fault closures and intersecting-fault-controlled fault closures. The spatial configuration of fault-related traps is influenced by the segmented growth of faults. Segments of faults with similar dip orientations control the formation of hanging-wall fault closures, whereas segments between faults with opposite dip orientations give rise to fault nose structures, consequently controlling the development of footwall closures.

Based on structural modeling and the fault-reservoir database of the Banqiao area, the fault-controlled reservoir models can be categorized as follows: same-dip fault sealing reservoir model, reverse-dip fault sealing reservoir model, intersecting fault sealing reservoir model, and reactivation-controlled secondary reservoir model.

Data availability statement

The original contributions presented in the study are included in the article/supplementary material, further inquiries can be directed to the corresponding author.

Author contributions

Funding

Acknowledgments

Conflict of interest

Authors HaL, CZ and HoL were employed by Research Institute of Petroleum Exploration and Development. Authors WJ and XD were employed by PetroChina Dagang Oilfield Company.

The remaining authors declare that the research was conducted in the absence of any commercial or financial relationships that could be construed as a potential conflict of interest.

Publisher's note

All claims expressed in this article are solely those of the authors and do not necessarily represent those of their affiliated organizations, or those of the publisher, the editors and the reviewers. Any product that may be evaluated in this article, or claim that may be made by its manufacturer, is not guaranteed or endorsed by the publisher.

References

Bense, V. F., Gleeson, T., Loveless, S. E., Bour, O., and Scibek, J. (2013). Fault zone hydrogeology. *Earth-Sci. Rev.* 127, 171–192. doi:10.1016/j.earscirev.2013.09.008

Bergen, K. J., Johnson, P. A., de Hoop, M. V., and Beroza, G. C. (2019). Machine learning for data-driven discovery in solid Earth geoscience. *Science* 363 (6433), eaau0323. doi:10.1126/science.aau0323

Callahan, O. A., Eichhubl, P., Olson, J. E., and Davatzes, N. C. (2019). Fracture mechanical properties of damaged and hydrothermally altered rocks, dixie valley-stillwater fault zone, Nevada, USA. *J. Geophys. Res. Solid Earth* 124 (4), 4069–4090. doi:10.1029/2018JB016708

Chen, C. W., Han, G. M., and Ma, J. Y. (2017). Analysis of favorable reservoir facies in the I-oil group of banqiao slope in qikou sag. *Special Oil Gas Reservoirs* 24 (01), 49–52. doi:10.3969/j.issn.1006-6535.2017.01.010

Chen, S. Q., Li, H. X., and Wang, X. P. (2013). Obzecive evaluation of gas in Es3 fomation, banziao slope. *Mud Logging Eng.* 24 (03), 88–92. doi:10.3969/j.issn.1672-9803.2013.03.021

Chen, Y. (2019). *Structural characteristics of banqiao slope fault zone and its roles in formation of hydrocarbon reservoirs*. Beijing: China university of mining technology.

Chen, Y., Liu, H. T., Zhao, C. Y., and Jiang, W. Y. (2021). Tectonic deformation characteristics and fault system division of banqiao slope in qikou sag. *J. Henan Polytech. Univ. (Nat. Sci.* 40 (01), 43–54. doi:10.16186/j.cnki.1673-9787.2019100044

Chen, Y. L., and Zhang, Y. N. (2018). Study on informatization of engineering geology and automatic mapping technology. *Water Resour. Hydropower Eng.* 49 (04), 145–153. doi:10.13928/j.cnki.wrahe.2018.04.021

Chu, R. (2019). *A Study on reservoir controled by synthetic and antithetic faults in Qinan slope area of Bohai Bay Basin*. Northeast Petroleum University. doi:10.26995/d.cnki.gdqsc.2019.000166

Chu, R., Liu, H. T., Wang, H. X., Jiang, W. Y., and Fu, X. F. (2019). Differences of vertical hydrocarbon enrichment controlled by different types of faults_ a case study of Qi'nan slope of Qikou depression,Bohai Bay Basin. *Acta Pet. Sin.* 40 (08), 928–940. doi:10.7623/syx620190800}

Clark Burchfiel, B., King, R. W., Todosov, A., Kotzev, V., Durmurdzanov, N., Serafimovski, T., et al. (2006). GPS results for Macedonia and its importance for the tectonics of the Southern Balkan extensional regime. *Tectonophysics* 413 (3-4), 239–248. doi:10.1016/j.tecto.2005.10.046

Cloos, H. (1928). *Über antithetische bewegungen.* 19 (3), 246–251. doi:10.1007/BF01788519

Conneally, J., Childs, C., and Walsh, J. J. (2014). Contrasting origins of breached relay zone geometries. *J. Struct. Geol.* 58, 59–68. doi:10.1016/j.jsg.2013.10.010

Cukur, D., Krastel, S., Tomonaga, Y., Schmincke, H., Sumita, M., Meydan, A. F., et al. (2017). Structural characteristics of the Lake Van Basin, eastern Turkey, from high-resolution seismic reflection profiles and multibeam echosounder data: geologic and tectonic implications. *Int. J. Earth Sci.* 106 (1), 239–253. doi:10.1007/s00531-016-1312-5

Davis, G. H. (1999). *Structural geology of the Colorado Plateau region of southern Utah, Structural geology of the Colorado Plateau region of southern Utah, with special emphasis on deformation bands*. Geological Society of America. doi:10.1130/0-8137-2342-6.1

Deng, H., Wang, R., Xiao, Y., Guo, J., and Xie, X. (2008). Tectono-Sequence stratigraphic analysis in continental faulted basins. *Earth Sci. Front.* 15 (2), 1–7. doi:10.1016/S1872-5791(08)60024-X

Deng, Y. (2018). *Study on the coupling relationship between hydrocarbon source and reservoir in Banqiao slope area of Qiqikou sag*. Research Institute of Petroleum Exploration and Development.

Dubbini, M., Cianfarra, P., Casula, G., Capra, A., and Salvini, F. (2010). Active tectonics in northern Victoria Land (Antarctica) inferred from the integration of GPS data and geologic setting. *J. Geophys. Res.* 115 (B12). doi:10.1029/2009JB007123

Eichhubl, P., Davatzes, N. C., and Becker, S. P. (2009). Structural and diagenetic control of fluid migration and cementation along the Moab fault, Utah. *AAPG Bull.* 93 (5), 653–681. doi:10.1306/02180908080

Etiope, G., and Martinelli, G. (2002). Migration of carrier and trace gases in the geosphere; an overview. *Phys. Earth Planet* 129 (3-4), 185–204. doi:10.1016/S0031-9201(01)00292-8

Faulkner, D. R., Jackson, C. A. L., Lunn, R. J., Schlische, R. W., Shipton, Z. K., Wibberley, C. A. J., et al. (2010). A review of recent developments concerning the structure, mechanics and fluid flow properties of fault zones. *J. Struct. Geol.* 32 (11), 1557–1575. doi:10.1016/j.jsg.2010.06.009

Faulkner, D. R., Mitchell, T. M., Jensen, E., and Cembrano, J. (2011). Scaling of fault damage zones with displacement and the implications for fault growth processes. *J. Geophys. Res.* 116 (B5), B05403. doi:10.1029/2010JB007788

Feng, D. X. (2015). *Geometry and kinematics of transtensional tectonics and its roles in petroleum geology, huimin sag, bohai bay basin*. Beijing: China University of Geosciences. Available at: https://kns.cnki.net/KCMS/detail/detail.aspx?filename=1015385649.nh&dbname=CDFDTEMP

Fisher, Q. J., Casey, M., Harris, S. D., and Knipe, R. J. (2003). Fluid-flow properties of faults in sandstone; the importance of temperature history. *Geol. (Boulder)* 31 (11), 965–968. doi:10.1130/G19823.1

Fossen, H. (2010). Extensional tectonics in the North atlantic caledonides: a regional view. *Geol. Soc. Lond. Spec. Publ.* 335 (1), 767–793. doi:10.1144/SP335.31

Fossen, H. (2016). *Structural geology*. Cambridge University Press. doi:10.1017/9781107415096

Fu, X., Chen, Z., Yan, B., Yang, M., and Sun, Y. (2013). Analysis of main controlling factors for hydrocarbon accumulation in central rift zones of the Hailar-Tamtsag Basin using a fault-caprock dual control mode. *Sci. China Earth Sciences* 56 (8), 1357–1370. doi:10.1007/s11430-013-4622-5

Fu, X., Yan, L., Meng, L., and Liu, X. (2019). Deformation mechanism and vertical sealing capacity of fault in the mudstone caprock. *J. Earth Sci.-China* 30 (2), 367–375. doi:10.1007/s12583-018-0998-7

Fu, X. F., Dong, J., and Lv, Y. F. (2012a). Fault structural characteristics of Wuerxun-Beier depression in the hailar basin and their Reservoir-Controlling mechanismsism. *ACTA Geol. sin.* 86 (06), 877–889. doi:10.3969/j.issn.0001-5717.2012.06.003

Fu, X. F., Song, X. Q., Wang, H. X., Liu, H., Wang, S., and Meng, L. (2021). Comprehensive evaluation on hydrocarbon-bearing availability of fault traps in a rift basin: a case study of the Qikou sag in the Bohai Bay Basin, China. *Petroleum Explor. Dev.* 48 (4), 787–797. doi:10.1016/S1876-3804(21)60066-6

Fu, X. F., Sun, B., Wang, H. X., and Meng, L. D. (2015). Fault segmentation growth quantitative characterization and its application on sag hydrocarbon accumulation research. *J. China Univ. Min. Technol.* 44 (02), 271–281. doi:10.13247/j.cnki.jcumt.000170

Fu, X. F., Xu, P., Wei, C. Z., and Lv, Y. F. (2012b). Internal structure of normal fault zone and hydrocarbon migration and conservation. *Earth Sci. Front.* 19 (06), 200–212. CNKI:Sun:DXQY.0.2012-06-025.

Gong, L., Liu, B., Fu, X., Jabbari, H., Gao, S., Yue, W., et al. (2019). Quantitative prediction of sub-seismic faults and their impact on waterflood performance: bozhong 34 oilfield case study. *J. Petrol. Sci. Eng.* 172, 60–69. doi:10.1016/j.petrol.2018.09.049

Gurnis, M., Yang, T., Cannon, J., Turner, M., Williams, S., Flament, N., et al. (2018). Global tectonic reconstructions with continuously deforming and evolving rigid plates. *Comput. Geosci.-UK.* 116, 32–41. doi:10.1016/j.cageo.2018.04.007

Han, G. M., Mou, L. G., and Dong, Y. Q. (2020). Cenozoic fault characteristics and petroleum geological significance in Banqiao slope area of Qikou Depression. *Bull. Geol. Sci. Technol.* 39 (06), 1–9. doi:10.19509/j.cnki.dzkq.2020.0603

He, H. T., Fan, T. Z., Guo, X. Z., and Yang, T. (2021). Major achievements in oil and gas exploration of PetroChina during the 13th Five-Year Plan period and its development strategy for the 14th Five-Year Plan. *China Pet. Explor.* 26 (01), 17–30. doi:10.3969/j.issn.1672-7703.2021.01.002

Hu, C., Cai, Y., Liu, M., and Wang, Z. (2013). Aftershocks due to property variations in the fault zone: a mechanical model. *Tectonophysics* 588, 179–188. doi:10.1016/j.tecto.2012.12.013

Huang, L., Liu, C., Wang, Y., Xue, Y., and Zhao, J. (2016). Hydrocarbon accumulation in strike-slip fault restraining bends: new insights into the tectonic controls on the Penglai 19-3 and Penglai 25-6 oil fields, Tan-Lu fault zone, east China. *AAPG Bull.* 100 (08), 1239–1263. doi:10.1306/03041614086

Jia, N., Liu, C., Huang, L., Zhou, L., Zhang, S., and Li, D. (2021). Formation mechanism of the Beidagang uplift, bohai Bay Basin, eastern China: insights from apatite fission track analysis and seismic data. *J. Asian Earth Sci.* 219, 104898. doi:10.1016/j.jseaes.2021.104898

Jiang, D. P., Wang, W. Y., and Gao, X. (2016). Mechanism and model of fault controlling reservoir in terms of the internal structure of fault zones: examples from zhu i depression, pearl river mouth basin. *Geol. Sci. Technol. Inf.* 35 (04), 91–97. CNKI:Sun:DZKQ.0.2016-04-014.

Jing, L., Yuan, Z., and Xu, Y. (2021). Paleoseismic investigation of the recurrence behavior of large earthquakes on active faults. *Earth Sci. Front.* 28 (02), 211–231. doi:10.13745/j.esf.sf.2020.9.8

John, W., Graham, Y., and Juan, W. (1991). The importance of small-scale faulting in regional extension. *Nature* 351 (6325), 391–393. doi:10.1038/351391A0

Li, W. (2016). Analysis of sand body distribution and sand control mechanism in Banqiao slope area. *China Petroleum Chem. Industry(S1)* 24. CNKI:Sun:SYFG.0.2016-S1-021.

Liu, H. T. (2019). *Geological evaluation techniques and applications for complex fracture block oil and gas reservoirs*. China science publishing and media ltd.

Liu, Q., Song, Y., Jiang, L., Cao, T., Chen, Z., Xiao, D., et al. (2017). Geochemistry and correlation of oils and source rocks in Banqiao Sag, Huanghua Depression, northern China. *Int. J. Coal Geol.* 176-177, 49–68. doi:10.1016/j.coal.2017.04.005

Liu, S. R. (2020). *Evolution and formation mechanism and reservoir forming control of complex fault zones in Qikou Depression*. Northeast Petroleum University. doi:10.26995/d.cnki.gdqsc.2020.000932

Liu, W. (2022). Analysis and implication of the geological big data management in developed countries: take USA, UK, Australia and Canada as example. *Geol. J. China Univ.* 28 (02), 274–286. doi:10.16108/j.issn1006-7493.2020103

Luo, Q., and Huang, H. D. (2009). Research on seismic-petroleum accumulation science and its application. *Acta Pet. Sin.* 30 (06), 876–881. doi:10.6038/pg20130130

Ma, J. Y., Liu, P., and Chen, S. Q. (2010). Deep Structural-Stratigraphical feature and exploration potential in banqiao sag. *Nat. Gas. Geosci.* 21 (04), 601–605. CNKI:Sun:TDKX.0.2010-04-014.

Manzocchi, T. R. P. S. U., Ringrose, P. S., and Underhill, J. R. (1998). Flow through fault systems in high-porosity sandstones. *Geol. Soc. Publ.* 127 (1), 65–82. doi:10.1144/GSL.SP.1998.127.01.06

McGill, G. E., Schultz, R. A., and Moore, J. M. (2000). Fault growth by segment linkage: an explanation for scatter in maximum displacement and trace length data from the Canyonlands grabens of SE Utah: discussion. *J. Struct. Geol.* 22 (1), 135–140. doi:10.1016/s0191-8141(99)00136-4

Morley, C. K., Gabdi, S., and Seusutthiya, K. (2007). Fault superimposition and linkage resulting from stress changes during rifting: examples from 3D seismic data, Phitsanulok Basin, Thailand. *J. Struct. Geol.* 29 (4), 646–663. doi:10.1016/j.jsg.2006.11.005

Peacock, D. (2000). 3-D structural geology. *Earth - Sci. Rev.* 51 (1), 213–214. doi:10.1007/978-3-662-03912-0

Peng, H. J., Pang, X. Q., and Li, H. B. (2016). Quantitative evaluation of control of faults on hydrocarbon accumulation and play fairway prediction in zhu i depression of pearl river mouth basin. *Geoscience* 30 (06), 1318–1328. doi:10.3969/j.issn.1000-8527.2016.06.014

Peng, J., Wei, A., Sun, Z., Chen, X., and Zhao, D. (2018). Sinistral strike slip of the zhangjiakou-penglai Fault and its control on hydrocarbon accumulation in the northeast of shaleitian bulge, bohai Bay Basin, east China. *Petroleum Explor. Dev.* 45 (2), 215–226. doi:10.1016/S1876-3804(18)30025-9

Pfunt, H., Houben, G., and Himmelsbach, T. (2016). Numerical modeling of fracking fluid migration through fault zones and fractures in the North German Basin. *Hydrogeol. J.* 24 (6), 1343–1358. doi:10.1007/s10040-016-1418-7

Qu, Z. P. (2020). Transtensional fault activity evaluation and its control on hydrocarbon accumulation: a case study in Cenozoic Dongying Sag. *Fault-Block Oil Gas Field.* 27(04), 443–447.doi:10.6056/dkyqt202004007

Reber, J. E., Cooke, M. L., and Dooley, T. P. (2020). What model material to use? A Review on rock analogs for structural geology and tectonics. *Earth-Sci. Rev.* 202, 103107. doi:10.1016/j.earscirev.2020.103107

Reeve, M. T., Bell, R. E., Duffy, O. B., Jackson, C. A. L., and Sansom, E. (2015). The growth of non-colinear normal fault systems; what can we learn from 3D seismic reflection data? *J. Struct. Geol.* 70, 141–155. doi:10.1016/j.jsg.2014.11.007

Schueller, S., Braathen, A., Fossen, H., and Tveranger, J. (2013). Spatial distribution of deformation bands in damage zones of extensional faults in porous sandstones: statistical analysis of field data. *J. Struct. Geol.* 52, 148–162. doi:10.1016/j.jsg.2013.03.013

Schultz, R. A. (2019). *Geologic fracture mechanics[M]*. Cambridge University Press. doi:10.1017/9781316996737

Song, F., Su, N., Yang, S., Yao, R., and Chu, S. (2018). Sedimentary characteristics of thick layer lacustrine beach-bars in the cenozoic banqiao sag of the bohai Bay Basin, east China. *J. Asian Earth Sci.* 151, 73–89. doi:10.1016/j.jseaes.2017.10.026

Song, F., Su, N. N., and Yao, R. X. (2016). Cenozoic fault structural characteristics and reservoir forming model of Banqiao slope. *J. Southwest Petroleum Univ. Nat. Sci. Ed.* 38 (02), 49–58. doi:10.11885/j.issn.16745086.2014.05.13.01

Tang, L., Huang, T., Jin, W., Lü, Z., He, C., Ning, F., et al. (2009). Differential deformation and hydrocarbon accumulation in the superimposed basins. *Earth Sci. Front.* 16 (4), 13–22. doi:10.1016/S1872-5791(08)60099-8

Wang, H. Y. (2020). *Research on fault system and reservoir control in the Banqiao area, Qikou Sag*. Northeast Petroleum University. doi:10.26995/d.cnki.gdqsc.2020.000928

Wang, X. L. (2008). *The regional tectonic characteristic of Banqiao-Beidagang structural zone and its constraints on oil and gas reservoir*. China university of petroleum. doi:10.7666/d.y1362795

Wang, Y. N. (2021). *Study on the differences of hydrocarbon accumulation and enrichment between deep and shallow layers in Banqiao Sag*. China university of petroleum-beijing. doi:10.27643/d.cnki.gsybu.2021.000667

Wang, J. C., Fu, D. L., and Yin, L. L. (2018). Study on the discrimination of reservoir fluid properties in Banqiao slope of Qikou depression. *Urban Geol.* 13 (03), 102–106. CNKI:Sun:CSDZ.0.2018-03-016.

Wang, Z. H., Hao, M., Zhang, J. L., and Li, K. X. (2020). Study of petroleum basin geological information system on 3D visualization. *J. Geomatics* 45 (02), 64–68. doi:10.14188/j.2095-6045.2018258

Wang, Z. S., Chen, C. W., and Han, G. M. (2017). Rotate-tilt slope zone structures-sedimentary evolution and petroleum geologic significance: a case study of Banqiao Slope of Qikou Sag, Bohai Bay Basin. *Nat. Gas. Geosci.* 28 (11), 1650–1656. doi:10.11764/j.issn.1672-1926.2017.09.007

Wei, H., Liu, J., and Meng, Q. (2010). Structural and sedimentary evolution of the southern Songliao Basin, northeast China, and implications for hydrocarbon prospectivity. *AAPG Bull.* 94 (4), 533–566. doi:10.1306/09080909060

Wu, T. T., Wu, Z., Wang, W. Y., and Cai, S. (2019). Application of big data to reservoir controlling of different faults taking zhuI depression as an example. *J. Guangdong Univ. Petrochem. Technol.* 29 (03), 1–4. doi:10.3969/j.issn.2095-2562.2019.03.001

Xie, Z. H., Luo, J. S., and Liu, Z. L. (2015). Fault re-active and reservoir-controlling of xujiaweizi fault depression, songliao basin. *Geol. Rev.* 61 (06), 1332–1346. doi:10.16509/j.georeview.2015.06.012

Xie, Z. J. (2020). *Study on seismic activities in seismic zoning of China's seas and adjacent.* Institute of Engineering Mechanics, China Earthquake Administration. doi:10.27490/d.cnki.ggjgy.2020.000010

Yin, L. L., Shi, Q. R., and Tang, L. L. (2019). A study of the lower limit of effective reservoir on the banqiao slope. *Acta Geol. Sichuan* 39 (01), 61–64. doi:10.3969/j.issn.1006-0995.2019.01.014

Yuan, B., Qun, L., and Chao, W. (2013). Seismic-petroleum accumulation science and its application. *Prog. Geophys.* 28 (01), 280–286. doi:10.6038/pg20130130

Yuan, X. P., Leroy, Y. M., and Maillot, B. (2020). Control of fluid pressures on the formation of listric normal faults. *Earth Planet. Sc. Lett.* 529, 115849. doi:10.1016/j.epsl.2019.115849

Zelilidis, A., Piper, D. J. W., Vakalas, I., Avramidis, P., and Getsos, K. (2003). Oil and gas plays in Albania: do equivalent plays exist in Greece? *J. Petrol. Geol.* 26 (1), 29–48. doi:10.1111/j.1747-5457.2003.tb00016.x

Zhao, X., Jin, F., Li, Y., Wang, Q., Zhou, L., Lyu, Y., et al. (2016b). Slope belt types and hydrocarbon migration and accumulation mechanisms in rift basins. *Petroleum Explor. Dev.* 43 (6), 915–924. doi:10.1016/S1876-3804(16)30110-0

Zhao, X. Z., Jin, F. M., Li, Y. B., Wang, Q., Zhou, L., Lyu, Y., et al. (2016a). Slope belt types and hydrocarbon migration and accumulation mechanisms in rift basins. *Petroleum Explor. Dev.* 43 (06), 915–924. doi:10.1016/s1876-3804(16)30110-0

Zhao, X. Z., Liu, G. D., and Jin, F. M. (2015). Distribution features and pattern of effective source rock in small faulted lacustrine basin: a case study of the Lower Cretaceous in Erlian Basin. *Acta pet. sin.* 36 (6), 641–652. doi:10.7623/syxb201506001

Zhou, L. H., Chen, C. W., and Han, G. M. (2018). Sedimentary characteristics and distribution patterns of hyperpycnal flow in rifted lacustrine basins:a case study on lower Esl of Banqiao slope in Qikou sag. *China Pet. Explor.* 23 (04), 11–20. doi:10.3969/j.issn.1672-7703.2018.04.002

Zhou, P. G., Mao, J. G., and Hou, S. S. (2007). The design and construction of landslide warning system based on Web-GIS. *Earth Sci. Front.* (06), 38–42. doi:10.3321/j.issn:1005-2321.2007.06.006

Zhu, Y., Liu, S., Zhang, B., Gurnis, M., and Ma, P. (2021). Reconstruction of the cenozoic deformation of the bohai bay basin, north China. *Basin Res.* 33 (1), 364–381. doi:10.1111/bre.12470

Zhu, Y. B. (2020). *Quantitative reconstruction of the cenozoic deformation of the bohai Bay Basin.* Beijing: North China, China University of Geosciences. doi:10.27493/d.cnki.gzdzy.2020.000757